EUROPEAN RESPIRATORY *journal*

FLAGSHIP SCIENTIFIC JOURNAL OF ERS

Early View

Original article

Genetic Landscape of Adult Langerhans Cell Histiocytosis with Lung Involvement

Fanélie Jouenne, Sylvie Chevret, Emmanuelle Bugnet, Emmanuelle Clappier, Gwenaël Lorillon, Véronique Meignin, Aurélie Sadoux, Shannon Cohen, Alain Haziot, Alexandre How-Kit, Caroline Kannengiesser, Céleste Lebbé, Dominique Gossot, Samia Mourah, Abdellatif Tazi

Please cite this article as: Jouenne Félie, Chevret S, Bugnet E, *et al*. Genetic Landscape of Adult Langerhans Cell Histiocytosis with Lung Involvement. *Eur Respir J* 2019; in press (https://doi.org/10.1183/13993003.01190-2019).

Genetic Landscape of Adult Langerhans Cell Histiocytosis with Lung Involvement

Fanélie Jouenne,[1,2] Sylvie Chevret,[3,4] Emmanuelle Bugnet,[5] Emmanuelle Clappier,[6,7] Gwenaël Lorillon,[5] Véronique Meignin,[8] Aurélie Sadoux,[2] Shannon Cohen,[9] Alain Haziot,[9] Alexandre How-Kit,[10] Caroline Kannengiesser,[11] Céleste Lebbé,[1,12] Dominique Gossot,[13] Samia Mourah,[1,2] and Abdellatif Tazi[1,5,*]

[1]Université de Paris, INSERM U976, Institut de Recherche Saint-Louis, Paris, France

[2]Assistance Publique-Hôpitaux de Paris, Hôpital Saint-Louis, Laboratoire de Pharmacogénomique, Paris, France

[3]Université de Paris, U1153 CRESS, Équipe de Recherche en Biostatistiques et Épidémiologie Clinique (ECSTRRA), Paris, France

[4]Assistance Publique-Hôpitaux de Paris, Hôpital Saint-Louis, Service de Biostatistique et Information Médicale, Paris, France

[5]Assistance Publique-Hôpitaux de Paris, Hôpital Saint-Louis, Centre National de Référence des Histiocytoses, Service de Pneumologie, Paris, France

[6]Assistance Publique-Hôpitaux de Paris, Hôpital Saint-Louis, Laboratoire d'Hématologie Biologique, Paris, France

[7]Université de Paris, INSERM U944, Institut de Recherche Saint-Louis, Paris, France

[8]Assistance Publique-Hôpitaux de Paris, Hôpital Saint-Louis, Service de Pathologie, INSERM UMR_S1165, Paris, France

[9]INSERM U1160, Institut de Recherche Saint-Louis, Paris, France

[10]Laboratoire de Génomique Fonctionnelle, Fondation Jean Dausset – CEPH, Paris, France

[11]Université de Paris, Assistance Publique-Hôpitaux de Paris, Hôpital Bichat, Laboratoire de Génétique, Paris, France

[12]Assistance Publique-Hôpitaux de Paris, Hôpital Saint-Louis, Département de Dermatologie, Paris, France

[13]Institut du Thorax Curie-Montsouris, Département Thoracique, Institut Mutualiste Montsouris, Paris, France

[*]Corresponding author

Abdellatif Tazi

Service de Pneumologie, Hôpital Saint-Louis, 1 Avenue Claude Vellefaux, 75475, Paris cedex 10, France

E-mail: abdellatif.tazi@aphp.fr

Take-home message

MAPK alterations are present in most lesions from adult pulmonary LCH patients. In patients with refractory progressive disease, the identification of these alterations, including *BRAF* deletions, is important to guide the choice of targeted treatment.

Abstract

The clinical significance of the *BRAF*^{V600E} mutation in adult Langerhans cell histiocytosis (LCH), including pulmonary LCH (PLCH), is not well understood. Similarly, the spectrum of molecular alterations involved in adult LCH has not been fully delineated. To address these issues, we genotyped a large number of adult LCH biopsies and searched for an association of identified molecular alterations with clinical presentation and disease outcome.

Biopsies from 117 adult LCH (83 PLCH) patients (median age 36.4 years, 56 females, 38 multisystem disease, 79 single system disease, 65 current smokers) were genotyped for the *BRAF*^{V600E} mutation. In 69 cases, LCH lesions were also genotyped by whole-exome or targeted gene panel next-generation sequencing. Cox models were used to estimate the association of baseline characteristics with the hazard of LCH progression.

MAPK pathway alterations were detected in 59 (86%) cases: *BRAF*^{V600E} mutation (36%), *BRAF*$^{N486\_P490}$ deletion (28%), *MAP2K1* mutations (15%), and isolated *NRAS*^{Q61} mutations (4%), while *KRAS* mutations were virtually absent in PLCH lesions. The *BRAF*^{V600E} mutation was not associated with LCH presentation at diagnosis, including smoking status and lung function, in PLCH patients. *BRAF*^{V600E} status did not influence the risk of LCH progression over time.

Thus, MAPK alterations are present in most lesions from adult LCH patients, particularly in PLCH. Unlike what was reported in paediatric LCH, *BRAF*^{V600E} genotyping did not provide additional information on disease outcome. The search for alterations involved in the MAPK pathway, including *BRAF* deletions, is useful for guiding targeted treatment in selected patients with refractory progressive LCH.

Introduction

Langerhans cell histiocytosis (LCH) is an inflammatory myeloid neoplasia characterised by accumulation in involved tissues of abnormal cells believed to be of the monocyte/macrophage lineage that harbour pathogenic mutations activating the mitogen-activated protein kinase (MAPK) pathway [1]. LCH can affect patients of all ages, from neonates to the elderly, and it has a wide spectrum of clinical presentations and variable outcomes. In adults, lung involvement (pulmonary LCH) is commonly observed as part of multisystem (MS) disease or as an isolated LCH localization and occurs almost exclusively in young smoking adults [2]. The prognosis of pulmonary LCH (PLCH) may vary from spontaneous resolution to progressive severe disease leading to respiratory failure and, ultimately, to lung transplantation [2]. With the exception of pulmonary hypertension (PH), PLCH outcome is difficult to predict in an individual patient, and no reliable predictive factors have been identified [2].

Although the presence of the *BRAF*^{V600E} mutation in tissue biopsies from adult LCH has been widely reported [3-9], the impact of this mutation on clinical presentation and disease outcome, particularly in PLCH patients, remains elusive [7, 10]. Other alterations of the MAPK pathway (i.e., *MAP2K1* mutations) have been identified in LCH lesions, including the lung [6-9, 11-13]. In PLCH, we also identified *NRAS*^{Q61} mutations, either isolated or, more frequently, concurrent with *BRAF*^{V600E} mutations [7]. Consistent with this finding, Kamata et al. [14] reported that the expression of *KRAS*^{G12D} within myeloid lung cells in mice leads to PLCH-like lesions, although the presence of *KRAS* mutations has not been accurately assessed in PLCH lesions. Finally, in a substantial proportion of cases, the genomic alterations that could be involved in MAPK activation in adult LCH lesions remain unknown.

To address these issues, we took advantage of the large cohort of adult patients followed in our national reference centre to 1) widely genotype a large number of LCH biopsies and 2) search for an association of identified molecular alterations, particularly the *BRAF*^{V600E} mutation, with clinical presentation and disease outcome.

Material and methods

Patients and LCH samples

One hundred seventeen adult LCH patients (median age 36.4 years, 56 females, 79 with single system (SS) disease at diagnosis) were included in this study. Twenty-three of these patients were involved in a previous study [7]. Eighty-three (80%) patients had PLCH (isolated lung involvement n = 51; 65 current- and 16 ex-smokers).

This study population was part of 194 patients with histologically confirmed LCH seen at our centre during the same period (Figure 1) and were representative of the entire cohort (see details in Supplementary Tables 1 and 2).

Formalin-fixed paraffin-embedded (FFPE) LCH biopsies were available for all patients and were evaluated by haematoxylin and eosin (H&E) staining and anti-CD1a immunostaining (clone O10, Agilent Technologies, les Ulis, France). CD1a-positive areas were macrodissected for molecular biology analysis [7].

All tissue specimens were genotyped for the presence of *BRAF*^{V600E} and *NRAS* mutations. In 69 cases (50 PLCH), the size of the LCH biopsy allowed for comprehensive molecular analysis. Additionally, for 18 of these patients, frozen LCH tissue was also available for whole-exome sequencing (WES). Peripheral blood mononuclear cells (PBMCs) were available for 14

of them, which were used as a paired germline control for WES analysis. The remaining 4 frozen tissues without available PBMCs were analysed only for somatic hotspot alterations.

In 10 cases, CD11c-positive blood cells purified from thawed DMSO-frozen PBMCs by flow cytometry as previously described [15] were available for molecular analysis.

LCH presentation at the time of biopsy and the molecular genotyping performed on the tissue specimens are shown in Supplementary Figure 1 and Supplementary Table 3.

Because PLCH occurs almost exclusively in smokers [2], grossly normal lung tissue from 10 smoker patients, obtained at the time of thoracic surgery for localised lung carcinoma, was also genotyped for *KRAS*.

The study was performed in accordance with the Helsinki Declaration and was approved by the INSERM Institutional Review Board and Ethics Committee in Paris, France (IRB n°13-130). All patients provided informed consent for the use of their tissue specimens and clinical information for research.

Molecular genotyping techniques

DNA extraction was performed as previously described [7].

WES

Whole-exome capture was performed on the genomic platform of the IMAGINE Institute (Paris, France) using the SureSelect Human All Exon 58 Mb V6 Kit (Agilent Technologies) [16]. Sequencing was conducted on the Illumina HiSeq 2500 platform (Illumina, San Diego, CA, USA). Variants were annotated and analysed using the Polyweb software interface (http://www.polyweb.fr/) and Alamut software (Interactive Biosoftware, Rouen, France). The

mean depth of coverage obtained was 142X (range 92.60X - 257X, mean 124X for PBMCs and 155X for tissue biopsies), with > 98% and > 96% of the targeted exonic bases covered by at least 15 and 30 independent sequencing reads, respectively (see details in Supplementary Methods).

Gene panel next-generation sequencing

A custom-designed next-generation sequencing (NGS) panel of 74 genes involved in MAPK, phosphoinositide 3-kinase, cell cycle, and tyrosine kinase receptor signalling pathways [12, 13, 17] was used for the comprehensive genotyping of LCH tissue biopsies (Supplementary Table 4). In addition, a custom-designed NGS panel of 78 genes involved in myeloid haematological disorders [18] was performed on frozen LCH specimens (Supplementary Table 5).

Pyrosequencing

BRAF^{V600E} and *NRAS*$^{G12/G13/Q61}$ genotyping was also performed as previously described [7]. *BRAF* exon 12 deletions described in paediatric LCH [19] were searched using a specific custom-designed pyrosequencing assay (detailed in Supplementary Methods and Supplementary Figure 2).

Enhanced-Ice-COLD-PCR

The sensitive detection of mutations in *BRAF* codon 600; *NRAS* codons 12, 13 and 61; and *KRAS* codons 12 and 13 was performed by E-Ice-COLD-PCR [7].

Data collection

Data on patient demographics, smoking habits, clinical symptoms and signs, LCH localisation and lung function tests at the time of diagnosis and during follow-up, as well as systemic treatments for LCH received by the patients during the study, were retrieved from the database. Patients were categorised as having SS or MS disease according to the Histiocyte Society criteria [20].

During follow-up, based on the global outcome of their disease, LCH patients were classified as having nonactive disease (NAD) if all signs and symptoms had resolved. Otherwise, they were classified as having active disease (AD). AD was further subdivided into better, stable or worse [20]. All patients who received systemic treatment for their LCH were categorised as having progressive disease.

The outcome of LCH lung involvement was based on variations over time of lung function tests and/or the occurrence of a new pneumothorax during follow-up [21]. Lung volumes were evaluated by plethysmography, forced expiratory volume in one second (FEV_1) and forced vital capacity (FVC) by the flow-volume curve. Diffusing capacity of carbon monoxide (D_{LCO}) was measured using the single-breath method. The predictive values were determined as previously described [21]. A worsening of lung function was defined as a decrease of 15% or more in FEV_1, FVC and/or D_{LCO} values compared with baseline values [21]. Patients who developed chronic respiratory failure, who were on long-term supplemental oxygen and/or who had developed PH were classified as having progressive lung disease. Noteworthy, MS LCH patients with lung involvement could have progressed, either because of the global outcome of their disease, and/or because of lung progression.

At the time of the last follow-up, the patient status (alive vs. deceased) was recorded.

Statistical analysis

Summary statistics that included the mean and standard deviation or median with interquartile range (IQR) or percentages were calculated.

The distribution of right-censored end points (time to progression or death) was estimated by the Kaplan-Meier method. Univariable Cox models were used to estimate the strength of the association of baseline characteristics, including mutations, as measured by the hazard ratio (HR) on the hazard of progression. Variables selected with the outcome at the 5% level were introduced into a multivariable Cox model. Model selection was performed using a stepwise procedure based on the Akaike information criterion.

Statistical analyses were performed using SAS (SAS Inc., Cary, NC, USA) and R (https://www.R-project.org/) software. All tests were two-sided, with p-values of 0.05 denoting statistical significance.

Results

Landscape of molecular abnormalities detected in LCH lesions

WES analysis, performed on frozen tumour lesions from 14 LCH (11 PLCH) patients with a matched PBMC specimen, revealed an average number of 14 somatic mutations targeting an average of 13 genes (Table 1). Four additional frozen lesions were analysed for somatic hotspot alterations.

A *BRAF*^{V600E} mutation or *BRAF*$^{N486\_P490}$ deletion was detected in 14 lesions, and *MAP2K1* alterations were detected in two lesions. Additionally, *NRAS*^{G12D} and *NRAS*^{Q61K} mutations were identified in one and 3 lesions, respectively, concurrently with a *BRAF*^{V600E}

mutation. Hence, a genomic alteration activating the MAPK pathway was identified in 16 out of 18 (89%) LCH cases.

Among the additional mutations identified, two missense mutations predicted to be deleterious (based on the algorithms used) were detected in two distinct lesions, i.e., *NT5C1B-RDH14*^{R191H} and *CP*^{G895A}, and 3 frameshift alterations were detected in 3 other lesions, i.e., a small insertion in *CIC* and *UNC5B* and a small deletion in *DTHD1* (Table 1).

Because there is a known association of myeloid malignancies with a histiocytic disorder related to LCH, known as Erdheim-Chester disease (ECD) [22], we investigated 17 of these 18 frozen LCH biopsies using a custom-designed NGS panel for myeloid disorders. In one LCH lesion (skin biopsy), two pathogenic mutations were identified in *TET2* (Q114X, variant allele frequency (VAF) 12% and G1370R, VAF 5%), as well as an in-frame internal tandem duplication in *FLT3* (*FLT3*-ITD), concurrently present with *BRAF*^{V600E} and *NRAS*^{G12D} mutations.

Since the identified mutations mainly involved the MAPK pathway, we extended the genomic analysis to a larger series of LCH lesions using a custom-designed NGS panel of 74 genes including MAPK pathway genes. Among the 69 (50 PLCH) LCH lesions analysed (including the 18 lesions sequenced by WES), a *BRAF* alteration was identified in 46 (67%) cases and consisted of 25 (36%) *BRAF*^{V600E} mutations, 20 (29%) *BRAF*$^{N486\_P490}$ deletions (concurrently present with a *BRAF*^{V600E} mutation in one case) and one *BRAF*^{G469A} mutation (lung biopsy). The *BRAF*^{G469A} mutation was previously identified in *BRAF*-mutated lung adenocarcinomas [23]. This mutation belongs to class 2 of the *BRAF* mutants and is insensitive to the BRAF inhibitor vemurafenib [24].

MAP2K1 alterations were detected in 10 (14.5%) lesions and consisted of 6 *MAP2K1* mutations and 4 *MAP2K1* deletions. All mutations were localised to exons 2 and 3, encoding the

autoregulatory domain and the catalytic core of MAP2K1 (also called MEK1). Five of these mutations are activating: Q56P [25], K57N [26], E102_I103 deletion [12], G128D and C121S [13]. An R108W mutation, not functionally evaluated previously, was identified in one case. This mutation, located in the protein kinase catalytic domain, was predicted to be deleterious by 3/3 algorithms and was shown by peptide arrays to have a critical role on the surface of MEK1 for tubulin interaction [27]. Another case harboured an undescribed L101Dfs*18 frameshift deletion, which generates a stop codon 18 positions downstream.

Isolated *NRAS*^{Q61} mutations were observed in 3 cases (two lung and one bone tissue). In addition, 11 other lesions (lung n=8, skin n=3) harboured *NRAS* mutations (*NRAS*^{G12D}, n=2; *NRAS*^{Q61}, n=9) in association with other alterations (*BRAF*^{V600E} in 9 cases). Finally, one isolated *KRAS*^{G12S} mutation was observed in a skin biopsy, and only one lung biopsy sample harboured a *KRAS*^{G12D} mutation, which was concurrently identified with a *BRAF*^{V600E} and an *NRAS*^{Q61R} mutation. No *KRAS*^{G12D} mutations were identified by NGS in the control lung tissue obtained from 10 smokers. All these findings were confirmed by at least one additional genotyping technique (pyrosequencing and/or E-Ice-COLD-PCR).

Overall, a pathogenic alteration of the MAPK pathway was observed in 59 (86%) of the 69 tested lesions (Table 2; Figures 2 and 3). More precisely, 44 of the 50 PLCH (88%) patients' lesions contained a MAPK alteration. Several other mutations that could potentially be involved in LCH pathogenesis were identified concurrently with MAPK alterations (Table 2 and Figure 2) (detailed in Supplementary Table 6). The prevalence of the identified molecular alterations did not significantly differ according to the site of LCH biopsy (p=0.60).

No MAPK alterations could be identified in purified CD11c+ blood cells available from 10 (6 MS) LCH patients, although 8/10 paired lesions harboured genomic alterations.

Correlation between MAPK alterations and clinical features

For the 69 LCH patients whose lesions were widely genotyped, no difference in clinical features was identified according to the different MAPK alterations, both at diagnosis and during follow-up. The cumulative incidence of LCH progression during the study period was not different according to the different mutations identified (Figure 4, p=0.6, Gray test).

Because the *BRAF*^{V600E} mutation is a driving mutation in LCH and was shown to be correlated with LCH severity in paediatric LCH [15, 28], we specifically evaluated the clinical impact of this mutation. Of note, in other MAPK related diseases, particularly melanoma, this mutation was shown to be an independent prognostic factor, whereas other MAPK activating mutations did not have the same prognostic impact [29, 30]. For this purpose, 48 additional patients whose LCH tissues were genotyped for *BRAF*^{V600E} (mutated in 37.5%) were included in this analysis. The characteristics of LCH at diagnosis were comparable to those of the 69 patients whose lesions were widely genotyped, with the exception that the latter were somewhat younger (p=0.051) and had less frequently bone involvement (p=0.04). Considering the entire study population (n=117), no association was found between *BRAF*^{V600E} status and LCH presentation at diagnosis (Table 3).

Among the 83 PLCH patients, no difference in smoking status (p=0.42) or the proportion of pneumothorax (p=0.29) was identified according to the presence or absence of the *BRAF*^{V600E} mutation in tissue lesions. Lung function at diagnosis was available for 73 (88%) patients in comparable proportions in patients with and without the *BRAF*^{V600E} mutation. The proportion of restrictive pattern, airflow obstruction or impairment of D_{LCO} (<80% of predicted values) was similar between the two groups of patients (p=0.088, p=0.44 and p=0.11, respectively).

Patients were followed for a median time of 59.5 months [IQR, 32-117.5]. Based on the global outcome of LCH, overall 70 (60%) patients experienced a progression of LCH during the study period that consisted in 18 progressions in LCH patients without pulmonary involvement, and in 52 patients with LCH lung localisation at diagnosis. Noteworthy, only 38 of these 52 progressions were related to a lung progression in PLCH patients. Thirty-seven patients needed systemic LCH treatment (consisting mainly in corticosteroids associated to vinblastine and/or cladribine). A comparable proportion of patients with and without *BRAF*^{V600E} mutated lesions received systemic LCH treatment (p=0.21 Fisher exact test). Seven (6%) patients died (5 linked to LCH), and two received transplants due to lung involvement. The probability of disease progression over time was similar regardless of the *BRAF*^{V600E} status of the lesions (Figure 5a).

Among the PLCH population, 38 (46%) patients experienced lung progression (including 10 patients with respiratory failure, long-term oxygen or PH). *BRAF*^{V600E} status was not associated with lung involvement outcome (Figure 5b, p=0.55, Gray test).

In the univariable analysis, an older age at diagnosis was associated with an increased risk of disease progression in patients [HR 1.37/decade, 95% CI (1.04-1.80); p=0.027], including the group of PLCH patients [HR 1.37, 95% CI (1.02-1.80); p=0.027]. Additionally, the presence of airflow obstruction was associated with lung progression (Supplementary Table 7). In the multivariable analysis, only the presence of airflow obstruction remained associated with an increased risk of lung progression [HR 2.00, 95% CI (1.05-3.84); p=0.036] (Table 4).

Discussion

In this study, we found the following salient results: 1) MAPK alterations were present in nearly 90% of the LCH lesions; 2) besides *BRAF*^{V600E} mutations, *BRAF*$^{N486\_P490}$ deletions were

identified in a substantial proportion of cases; 3) *KRAS* mutations were virtually absent from PLCH lesions; and 4) *BRAF*^{V600E} mutation was not associated with either the initial presentation or the outcome of PLCH.

MAPK alterations were present in 86% of the LCH biopsies evaluated by NGS, and only a small minority of cases were found to be wild-type. Moreover, because we did not perform RNA sequencing on tissue specimens, we cannot exclude the possibility that additional MAPK alterations, such as *BRAF* kinase fusion, were missed [19, 31]. Thus, in the vast majority of adult LCH cases, particularly PLCH cases, the disease appears to be driven by genomic alterations involving the MAPK pathway.

The *BRAF*^{V600E} mutation was identified in 36% of the cases and in similar percentages among the subgroups of patients whose lesions were evaluated by NGS or by gene-specific genotyping. This frequency of *BRAF*^{V600E} mutations was significantly lower than the 64% observed by Chakraborty et al. [19] in paediatric LCH, but close to the 42% reported by Heritier et al. in paediatric LCH with lung involvement [28]. Conversely, we identified *BRAF*$^{N486\_P490}$ deletions in up to 30% of our cases, in similar proportions by WES and a dedicated pyrosequencing assay, which is much higher than the 6% frequency reported in paediatric LCH [19]. In contrast, the *MAP2K1* alterations observed in this series occurred in a similar proportion as that reported in paediatric LCH (14.5% and 12%, respectively) [19]. Finally, no isolated *KRAS* mutations were identified in PLCH; thus, our results do not support a role for this mutation in the development of PLCH lesions, unlike what has been recently suggested in a murine model in which a *KRAS* mutation was induced in lung myeloid cells [14].

The identification of these different MAPK alterations has an impact on MAPK-targeted treatment. While the *BRAF*^{V600E} mutation is sensitive to BRAF inhibitors [32, 33], *BRAF*$^{N486\_P490}$

deletion was shown to be relatively resistant to "first-generation" *BRAF*^{V600E} inhibitors but sensitive to MEK inhibitors [19]. Similarly, LCH patients whose lesions harbour *MAP2K1* mutations were shown to respond to MEK inhibitors [19, 34-36].

In this series of exclusively LCH cases, only one lesion contained molecular alterations involved in myeloid haematological disorders, i.e., *TET2* mutation as well as an in-frame duplication in *FLT3*, concurrently with *BRAF*^{V600E} and *NRAS*^{G12D} mutations. *TET2* is widely involved in haematological malignancies and in clonal haematopoiesis of indeterminate potential [37, 38]. The in-frame duplication in *FLT3* found here corresponds to a recurrent alteration observed in acute myeloid leukaemia [39]. At more than 4 years of follow-up, our patient did not develop any haematological disorders. The rare observation of molecular alterations in myeloid neoplasms is contrary to what has been reported in ECD, which may be explained by the younger age of our patients compared with ECD patients [22].

An important result of this study in the clinical context is the absence of an association between the *BRAF*^{V600E} mutation (tested in all cases) and either the initial presentation or the outcome of the patients. This result contrasts with that found in paediatric LCH, in which the *BRAF*^{V600E} mutation was associated with recurrence, severity and resistance to first-line therapy [15, 28]. However, an important difference of adult LCH is that risk organ (i.e., liver, spleen, haematological system) involvement, which is associated with disease severity in paediatric LCH [1], is rarely present [20], as was the case in the present series.

In this large cohort of PLCH patients, we did not find any association between smoking and *BRAF*^{V600E} status, contrary to what has been previously suggested based on a small series of patients [5]. Importantly, the outcome of PLCH patients, based on lung function variations over time, was not influenced by the *BRAF*^{V600E} status of their lesions. The proportion of nearly 50%

of patients whose pulmonary involvement worsened during the study, in which patients were followed for a 6-year median time, was similar to the proportion that we previously observed at 5 years in a smaller retrospective multicentre study [40]. In contrast, airflow obstruction at diagnosis was a predictive factor of worsening of lung function during follow-up in this large cohort study in which the data were prospectively registered.

Although our study population was representative of all histologically confirmed adult LCH seen at our centre, it may not reflect patients with isolated mild PLCH for whom a surgical lung biopsy is not constantly performed. However, these patients with a presumptive diagnosis retained on a clinical and imaging basis, usually do not progress [2]. Thus, the findings of the present study are clinically meaningful. Similarly, because the LCH recruitment of our centre is oriented towards PLCH, the lack of clinical impact of the *BRAF*^{V600E} mutation found in this study needs to be confirmed in a series of adult LCH without lung involvement.

In summary, MAPK alterations are present in most lesions from adult LCH patients, particularly in PLCH. The search for alterations involved in MAPK pathway activation, including *BRAF*$^{N486\_P490}$ deletion, is important to guide the choice of targeted treatment in selected patients with refractory progressive LCH.

Acknowledgements

This study was supported by a grant from the Legs Poix Chancellerie des Universités de Paris, France. The authors thank C. Bole-Feysot, M. Zarhrate and M. Parisot from the Imagine Institute for WES genotyping. The authors are grateful to Dr. Omar Abdel-Wahab (Memorial Sloan Kettering Cancer Center, New York, USA) for his critical reading of the manuscript. The authors

thank M. Mao and E. Savariau (Assistance Publique-Hôpitaux de Paris; Service de Pneumologie, Hôpital Saint-Louis, Paris, France) for their technical assistance.

References

1. Allen CE, Merad M, McClain KL. Langerhans-Cell Histiocytosis. N Engl J Med 2018; 379: 856-868.
2. Vassallo R, Harari S, Tazi A. Current understanding and management of pulmonary Langerhans cell histiocytosis. Thorax 2017; 72: 937-945.
3. Badalian-Very G, Vergilio JA, Degar BA, MacConaill LE, Brandner B, Calicchio ML, Kuo FC, Ligon AH, Stevenson KE, Kehoe SM, Garraway LA, Hahn WC, Meyerson M, Fleming MD, Rollins BJ. Recurrent BRAF mutations in Langerhans cell histiocytosis. Blood 2010; 116: 1919-1923.
4. Chilosi M, Facchetti F, Calio A, Zamo A, Brunelli M, Martignoni G, Rossi A, Montagna L, Piccoli P, Dubini A, Tironi A, Tomassetti S, Poletti V, Doglioni C. Oncogene-induced senescence distinguishes indolent from aggressive forms of pulmonary and non-pulmonary Langerhans cell histiocytosis. Leuk Lymphoma 2014; 55: 2620-2626.
5. Roden AC, Hu X, Kip S, Parrilla Castellar ER, Rumilla KM, Vrana JA, Vassallo R, Ryu JH, Yi ES. BRAF V600E expression in Langerhans cell histiocytosis: clinical and immunohistochemical study on 25 pulmonary and 54 extrapulmonary cases. Am J Surg Pathol 2014; 38: 548-551.
6. Kamionek M, Ahmadi Moghaddam P, Sakhdari A, Kovach AE, Welch M, Meng X, Dresser K, Tomaszewicz K, Cosar EF, Mark EJ, Fraire AE, Hutchinson L. Mutually

exclusive extracellular signal-regulated kinase pathway mutations are present in different stages of multi-focal pulmonary Langerhans cell histiocytosis supporting clonal nature of the disease. Histopathology 2016; 69: 499-509.

7. Mourah S, How-Kit A, Meignin V, Gossot D, Lorillon G, Bugnet E, Mauger F, Lebbe C, Chevret S, Tost J, Tazi A. Recurrent NRAS mutations in pulmonary Langerhans cell histiocytosis. Eur Respir J 2016; 47: 1785-1796.
8. Alayed K, Medeiros LJ, Patel KP, Zuo Z, Li S, Verma S, Galbincea J, Cason RC, Luthra R, Yin CC. BRAF and MAP2K1 mutations in Langerhans cell histiocytosis: a study of 50 cases. Hum Pathol 2016; 52: 61-67.
9. Zeng K, Ohshima K, Liu Y, Zhang W, Wang L, Fan L, Li M, Li X, Wang Z, Guo S, Yan Q, Guo Y. BRAFV600E and MAP2K1 mutations in Langerhans cell histiocytosis occur predominantly in children. Hematol Oncol 2017; 35: 845-851.
10. Selway JL, Harikumar PE, Chu A, Langlands K. Genetic homogeneity of adult Langerhans cell histiocytosis lesions: Insights from BRAF(V600E) mutations in adult populations. Oncol Lett 2017; 14: 4449-4454.
11. Brown NA, Furtado LV, Betz BL, Kiel MJ, Weigelin HC, Lim MS, Elenitoba-Johnson KS. High prevalence of somatic MAP2K1 mutations in BRAF V600E-negative Langerhans cell histiocytosis. Blood 2014; 124: 1655-1658.
12. Chakraborty R, Hampton OA, Shen X, Simko SJ, Shih A, Abhyankar H, Lim KP, Covington KR, Trevino L, Dewal N, Muzny DM, Doddapaneni H, Hu J, Wang L, Lupo PJ, Hicks MJ, Bonilla DL, Dwyer KC, Berres ML, Poulikakos PI, Merad M, McClain KL, Wheeler DA, Allen CE, Parsons DW. Mutually exclusive recurrent somatic mutations in

MAP2K1 and BRAF support a central role for ERK activation in LCH pathogenesis. Blood 2014; 124: 3007-3015.

13. Nelson DS, van Halteren A, Quispel WT, van den Bos C, Bovee JV, Patel B, Badalian-Very G, van Hummelen P, Ducar M, Lin L, MacConaill LE, Egeler RM, Rollins BJ. MAP2K1 and MAP3K1 mutations in langerhans cell histiocytosis. Genes Chromosomes Cancer 2015; 54: 361-368.
14. Kamata T, Giblett S, Pritchard C. KRAS(G12D) expression in lung-resident myeloid cells promotes pulmonary LCH-like neoplasm sensitive to statin treatment. Blood 2017; 130: 514-526.
15. Berres ML, Lim KP, Peters T, Price J, Takizawa H, Salmon H, Idoyaga J, Ruzo A, Lupo PJ, Hicks MJ, Shih A, Simko SJ, Abhyankar H, Chakraborty R, Leboeuf M, Beltrao M, Lira SA, Heym KM, Bigley V, Collin M, Manz MG, McClain K, Merad M, Allen CE. BRAF-V600E expression in precursor versus differentiated dendritic cells defines clinically distinct LCH risk groups. J Exp Med 2014; 211: 669-683.
16. Thevenon J, Michot C, Bole C, Nitschke P, Nizon M, Faivre L, Munnich A, Lyonnet S, Bonnefont JP, Portes VD, Amiel J. RPL10 mutation segregating in a family with X-linked syndromic Intellectual Disability. Am J Med Genet A 2015; 167A: 1908-1912.
17. Cancer Genome Atlas N. Genomic Classification of Cutaneous Melanoma. Cell 2015; 161: 1681-1696.
18. Papaemmanuil E, Gerstung M, Bullinger L, Gaidzik VI, Paschka P, Roberts ND, Potter NE, Heuser M, Thol F, Bolli N, Gundem G, Van Loo P, Martincorena I, Ganly P, Mudie L, McLaren S, O'Meara S, Raine K, Jones DR, Teague JW, Butler AP, Greaves MF,

Ganser A, Dohner K, Schlenk RF, Dohner H, Campbell PJ. Genomic Classification and Prognosis in Acute Myeloid Leukemia. N Engl J Med 2016; 374: 2209-2221.

19. Chakraborty R, Burke TM, Hampton OA, Zinn DJ, Lim KP, Abhyankar H, Scull B, Kumar V, Kakkar N, Wheeler DA, Roy A, Poulikakos PI, Merad M, McClain KL, Parsons DW, Allen CE. Alternative genetic mechanisms of BRAF activation in Langerhans cell histiocytosis. Blood 2016; 128: 2533-2537.
20. Tazi A, Lorillon G, Haroche J, Neel A, Dominique S, Aouba A, Bouaziz JD, de Margerie-Melon C, Bugnet E, Cottin V, Comont T, Lavigne C, Kahn JE, Donadieu J, Chevret S. Vinblastine chemotherapy in adult patients with langerhans cell histiocytosis: a multicenter retrospective study. Orphanet J Rare Dis 2017; 12: 95.
21. Tazi A, de Margerie C, Naccache JM, Fry S, Dominique S, Jouneau S, Lorillon G, Bugnet E, Chiron R, Wallaert B, Valeyre D, Chevret S. The natural history of adult pulmonary Langerhans cell histiocytosis: a prospective multicentre study. Orphanet J Rare Dis 2015; 10: 30.
22. Papo M, Diamond EL, Cohen-Aubart F, Emile JF, Roos-Weil D, Gupta N, Durham BH, Ozkaya N, Dogan A, Ulaner GA, Rampal R, Kahn JE, Sene T, Charlotte F, Hervier B, Besnard C, Bernard OA, Settegrana C, Droin N, Helias-Rodzewicz Z, Amoura Z, Abdel-Wahab O, Haroche J. High prevalence of myeloid neoplasms in adults with non-Langerhans cell histiocytosis. Blood 2017; 130: 1007-1013.
23. Paik PK, Arcila ME, Fara M, Sima CS, Miller VA, Kris MG, Ladanyi M, Riely GJ. Clinical characteristics of patients with lung adenocarcinomas harboring BRAF mutations. J Clin Oncol 2011; 29: 2046-2051.

24. Yao Z, Yaeger R, Rodrik-Outmezguine VS, Tao A, Torres NM, Chang MT, Drosten M, Zhao H, Cecchi F, Hembrough T, Michels J, Baumert H, Miles L, Campbell NM, de Stanchina E, Solit DB, Barbacid M, Taylor BS, Rosen N. Tumours with class 3 BRAF mutants are sensitive to the inhibition of activated RAS. Nature 2017; 548: 234-238.

25. Choi YL, Soda M, Ueno T, Hamada T, Haruta H, Yamato A, Fukumura K, Ando M, Kawazu M, Yamashita Y, Mano H. Oncogenic MAP2K1 mutations in human epithelial tumors. Carcinogenesis 2012; 33: 956-961.

26. Marks JL, Gong Y, Chitale D, Golas B, McLellan MD, Kasai Y, Ding L, Mardis ER, Wilson RK, Solit D, Levine R, Michel K, Thomas RK, Rusch VW, Ladanyi M, Pao W. Novel MEK1 mutation identified by mutational analysis of epidermal growth factor receptor signaling pathway genes in lung adenocarcinoma. Cancer Res 2008; 68: 5524-5528.

27. Cao JN, Shafee N, Vickery L, Kaluz S, Ru N, Stanbridge EJ. Mitogen-activated protein/extracellular signal-regulated kinase kinase 1act/tubulin interaction is an important determinant of mitotic stability in cultured HT1080 human fibrosarcoma cells. Cancer Res 2010; 70: 6004-6014.

28. Heritier S, Emile JF, Barkaoui MA, Thomas C, Fraitag S, Boudjemaa S, Renaud F, Moreau A, Peuchmaur M, Chassagne-Clement C, Dijoud F, Rigau V, Moshous D, Lambilliotte A, Mazingue F, Kebaili K, Miron J, Jeziorski E, Plat G, Aladjidi N, Ferster A, Pacquement H, Galambrun C, Brugieres L, Leverger G, Mansuy L, Paillard C, Deville A, Armari-Alla C, Lutun A, Gillibert-Yvert M, Stephan JL, Cohen-Aubart F, Haroche J, Pellier I, Millot F, Lescoeur B, Gandemer V, Bodemer C, Lacave R, Helias-Rodzewicz Z, Taly V, Geissmann

F, Donadieu J. BRAF Mutation Correlates With High-Risk Langerhans Cell Histiocytosis and Increased Resistance to First-Line Therapy. J Clin Oncol 2016; 34: 3023-3030.

29. Barbour AP, Tang YH, Armour N, Dutton-Regester K, Krause L, Loffler KA, Lambie D, Burmeister B, Thomas J, Smithers BM, Hayward NK. BRAF mutation status is an independent prognostic factor for resected stage IIIB and IIIC melanoma: implications for melanoma staging and adjuvant therapy. Eur J Cancer 2014; 50: 2668-2676.

30. Leeksma AC, Taylor J, Wu B, Gardner JR, He J, Nahas M, Gonen M, Alemayehu WG, Te Raa D, Walther T, Hullein J, Dietrich S, Claus R, de Boer F, de Heer K, Dubois J, Dampmann M, Durig J, van Oers MHJ, Geisler CH, Eldering E, Levine RL, Miller V, Mughal T, Lamanna N, Frattini MG, Heaney ML, Zelenetz A, Zenz T, Abdel-Wahab O, Kater AP. Clonal diversity predicts adverse outcome in chronic lymphocytic leukemia. Leukemia 2019; 33: 390-402.

31. Zarnegar S, Durham BH, Khattar P, Shukla NN, Benayed R, Lacouture ME, Lavi E, Lyden DC, Diamond EL, Dunkel IJ, Abdel-Wahab O. Novel activating BRAF fusion identifies a recurrent alternative mechanism for ERK activation in pediatric Langerhans cell histiocytosis. Pediatr Blood Cancer 2018; 65: e26699.

32. Diamond EL, Subbiah V, Lockhart AC, Blay JY, Puzanov I, Chau I, Raje NS, Wolf J, Erinjeri JP, Torrisi J, Lacouture M, Elez E, Martinez-Valle F, Durham B, Arcila ME, Ulaner G, Abdel-Wahab O, Pitcher B, Makrutzki M, Riehl T, Baselga J, Hyman DM. Vemurafenib for BRAF V600-Mutant Erdheim-Chester Disease and Langerhans Cell Histiocytosis: Analysis of Data From the Histology-Independent, Phase 2, Open-label VE-BASKET Study. JAMA Oncol 2018; 4: 384-388.

33. Haroche J, Cohen-Aubart F, Emile JF, Maksud P, Drier A, Toledano D, Barete S, Charlotte F, Cluzel P, Donadieu J, Benameur N, Grenier PA, Besnard S, Ory JP, Lifermann F, Idbaih A, Granel B, Graffin B, Hervier B, Arnaud L, Amoura Z. Reproducible and Sustained Efficacy of Targeted Therapy With Vemurafenib in Patients With BRAFV600E-Mutated Erdheim-Chester Disease. J Clin Oncol 2015; 33: 411-418.

34. Lee LH, Gasilina A, Roychoudhury J, Clark J, McCormack FX, Pressey J, Grimley MS, Lorsbach R, Ali S, Bailey M, Stephens P, Ross JS, Miller VA, Nassar NN, Kumar AR. Real-time genomic profiling of histiocytoses identifies early-kinase domain BRAF alterations while improving treatment outcomes. JCI Insight 2017; 2: e89473.

35. Lorillon G, Jouenne F, Baroudjian B, de Margerie-Mellon C, Vercellino L, Meignin V, Lebbe C, Vassallo R, Mourah S, Tazi A. Response to Trametinib of a Pulmonary Langerhans Cell Histiocytosis Harboring a MAP2K1 Deletion. Am J Respir Crit Care Med 2018; 198: 675-678.

36. Diamond EL, Durham BH, Ulaner GA, Drill E, Buthorn J, Ki M, Bitner L, Cho H, Young RJ, Francis JH, Rampal R, Lacouture M, Brody LA, Ozkaya N, Dogan A, Rosen N, Iasonos A, Abdel-Wahab O, Hyman DM. Efficacy of MEK inhibition in patients with histiocytic neoplasms. Nature 2019; 567: 521-524.

37. Cancer Genome Atlas Research N, Ley TJ, Miller C, Ding L, Raphael BJ, Mungall AJ, Robertson A, Hoadley K, Triche TJ, Jr., Laird PW, Baty JD, Fulton LL, Fulton R, Heath SE, Kalicki-Veizer J, Kandoth C, Klco JM, Koboldt DC, Kanchi KL, Kulkarni S, Lamprecht TL, Larson DE, Lin L, Lu C, McLellan MD, McMichael JF, Payton J, Schmidt H, Spencer DH, Tomasson MH, Wallis JW, Wartman LD, Watson MA, Welch J, Wendl MC, Ally A, Balasundaram M, Birol I, Butterfield Y, Chiu R, Chu A, Chuah E, Chun HJ,

Corbett R, Dhalla N, Guin R, He A, Hirst C, Hirst M, Holt RA, Jones S, Karsan A, Lee D, Li HI, Marra MA, Mayo M, Moore RA, Mungall K, Parker J, Pleasance E, Plettner P, Schein J, Stoll D, Swanson L, Tam A, Thiessen N, Varhol R, Wye N, Zhao Y, Gabriel S, Getz G, Sougnez C, Zou L, Leiserson MD, Vandin F, Wu HT, Applebaum F, Baylin SB, Akbani R, Broom BM, Chen K, Motter TC, Nguyen K, Weinstein JN, Zhang N, Ferguson ML, Adams C, Black A, Bowen J, Gastier-Foster J, Grossman T, Lichtenberg T, Wise L, Davidsen T, Demchok JA, Shaw KR, Sheth M, Sofia HJ, Yang L, Downing JR, Eley G. Genomic and epigenomic landscapes of adult de novo acute myeloid leukemia. N Engl J Med 2013; 368: 2059-2074.

38. Genovese G, Kahler AK, Handsaker RE, Lindberg J, Rose SA, Bakhoum SF, Chambert K, Mick E, Neale BM, Fromer M, Purcell SM, Svantesson O, Landen M, Hoglund M, Lehmann S, Gabriel SB, Moran JL, Lander ES, Sullivan PF, Sklar P, Gronberg H, Hultman CM, McCarroll SA. Clonal hematopoiesis and blood-cancer risk inferred from blood DNA sequence. N Engl J Med 2014; 371: 2477-2487.

39. Dohner H, Estey E, Grimwade D, Amadori S, Appelbaum FR, Buchner T, Dombret H, Ebert BL, Fenaux P, Larson RA, Levine RL, Lo-Coco F, Naoe T, Niederwieser D, Ossenkoppele GJ, Sanz M, Sierra J, Tallman MS, Tien HF, Wei AH, Lowenberg B, Bloomfield CD. Diagnosis and management of AML in adults: 2017 ELN recommendations from an international expert panel. Blood 2017; 129: 424-447.

40. Tazi A, Marc K, Dominique S, de Bazelaire C, Crestani B, Chinet T, Israel-Biet D, Cadranel J, Frija J, Lorillon G, Valeyre D, Chevret S. Serial computed tomography and lung function testing in pulmonary Langerhans' cell histiocytosis. Eur Respir J 2012; 40: 905-912.

Tables

Table 1. Selection of variants detected by WES using the Polyweb interface for the 14 lesions analysed with a matched PBMCs control sample*.

GENE	Variation†	Type	Patient number (VAF)	Consequence	Description	Exon	Amino acid variant	Genomic variant	PolyPhen 2	SIFT
BRAF	7_140453136_A_T (rs113488022)	SNV	10 (10%), 23 (4%), 27 (1%), 56 (4%), 59 (2%), 103 (11%)	MS	v-raf murine sarcoma viral oncogene homolog B	15	V600E	c.1799T>A	Prob Dam	Del
BRAF	7_140477837_AATGTGACAGCACCTA_A	del	8 (2.5%), 16 (12%), 30 (4%), 31 (2%)	IF	v-raf murine sarcoma viral oncogene homolog B	12	LNVTAPT486LT	c.1457_1471del	-	-
CIC	19_42799295_A_AG	ins	67 (34%)	FS	capicua transcriptional repressor	20	Q1593QA	c.4778_4779ins	-	-
CP	3_148896396_C_G (rs139633388)	SNV	57 (10%)	MS	ceruloplasmin (ferroxidase)	16	G895A	c.2684G>C	Prob Dam	Del
DTHD1	4_36285990_TAAAC_T	del	57 (10%)	FS	death domain containing 1	1	KQ97X	c.289_292del	-	-
HMCN1	1_186086719_C_A (rs376333827)	SNV	57 (21%)	MS	hemicentin 1	77	L3938I	c.11812C>A	Poss Dam	Ben
MAP2K1	15_66729093_TCTGGA_T	del	2 (14%)	FS	Mitogen-Activated Protein Kinase Kinase 1	3	§L101Dfs*18	c.301_305del	-	-
MAP2K1	15_66729093_TGGAGAT_T	del	57 (7%)	IF	Mitogen-Activated Protein Kinase Kinase 1	3	LEIK 102LK	c.303_308del	-	-
NRAS	1_115256530_G_T (rs121913254)	SNV	10 (14%), 27 (4%), 59 (8%)	MS	V-Ras Neuroblastoma RAS Viral Oncogene Homolog	3	Q61K	c.181C>A	Poss Dam	Del
NT5C1B-RDH14	2_18765937_C_T	SNV	103 (15%)	MS	NT5C1B-RDH14 readthrough	4	R191H	c.572G>A	Prob Dam	Del
PCLO	7_82584553_C_A (rs202091944)	SNV	57 (17%)	MS	piccolo presynaptic cytomatrix protein	5	G1906C	c.5716G>T	Prob Dam	Ben
PPFIA2	12_81657159_T_C (rs368764392)	SNV	57 (15%)	MS	protein tyrosine phosphatase, receptor type, f polypeptide (PTPRF), interacting protein (liprin), alpha 2	31	K1189R	c.3566A>G	Ben	Del
UNC5B	10_73056470_G_GATATTCCAGC	ins	71 (50%)	FS	unc-5 homolog B (C. elegans)	15	I821IF	c.2460_2461ins	-	-

	TGCATACCACT CTGGCAGAGG TGAGGGAAGT CGGGGCCAC (rs879908823)									

*11 patients had PLCH at diagnosis.

†Variation: Chromosome_Genomic position_ Allele reference_ Allele mutated (rs number).

[§]fs*18: variant that causes a frameshift. The new reading frame ends on a downstream 18-position STOP codon.

Abbreviations: WES: whole-exome sequencing; PBMCs: peripheral blood mononuclear cells; VAF: variant allele frequency; SNV: single nucleotide variant; MS: missense; Prob Dam: probably damaging; Del: deleterious; del: deletion; IF: in-frame deletion; ins: insertion; FS: frameshift; Poss Dam: possibly damaging; Ben: benign.

Table 2. Results of genotyping of the 69 patients whose LCH lesions were widely genotyped by NGS and pyrosequencing for *BRAF* deletions*.

Patient	Predominant variant	Additional variants
1	*BRAF* V600E	
2	*MAP2K1* L101Dfs*18	
3*	*BRAF* N486_P490 deletion	
4*	*MAP2K1* C121S	
5*	*MAP2K1* R108W	*DUSP* D231N, *ERBB2* T791I
6*	*BRAF* N486_P490 deletion	
7*	*MAP2K1* G128D	*NRAS* Q61K
8*	*BRAF* N486_P490 deletion	
9*	WT	
10*	*BRAF* V600E	*NRAS* Q61K
11*	*MAP2K1* G128D	
12	*BRAF* V600E	
13*	*BRAF* N486_P490 deletion	
14*	WT	
15	*BRAF* N486_P490 deletion	
16*	*BRAF* N486_P490 deletion	
17*	*BRAF* V600E	*NRAS* Q61K
18*	*BRAF* V600E	*NRAS* Q61R, *ERBB4* R838X, *MET* S244F, *NOTCH1* c.6181-1G>A, *PPP6C* P296S
19*	WT	
20	*BRAF* V600E	*NRAS* Q61L, *EGFR* P753S
21*	*BRAF* N486_P490 deletion	
22*	*NRAS* Q61K	
23*	*BRAF* V600E	
24*	WT	
25*	*BRAF* V600E	
26*	*BRAF* V600E	
27*	*BRAF* V600E	*NRAS* Q61K
28	*BRAF* N486_P490 deletion	
29	WT	
30*	*BRAF* N486_P490 deletion	
31*	*BRAF* N486_P490 deletion	
32*	*BRAF* N486_P490 deletion	
33*	*BRAF* V600E	*NRAS* Q61R, *KRAS* G12D
34*	*BRAF* non V600E (G469A)	
35*	*MAP2K1* E102_I103 deletion	
36*	*BRAF* V600E	

37*	*BRAF* V600E	
38*	*MAP2K1* E102_I103 deletion	
39	*BRAF* V600E	
40*	*BRAF* V600E	*BRAF* N486_P490 deletion
41*	*BRAF* N486_P490 deletion	
42*	*BRAF* V600E	
43*	*BRAF* V600E	
44*	*BRAF* V600E	
45*	*BRAF* V600E	
46*	*BRAF* N486_P490 deletion	
47	*BRAF* V600E	*NRAS* G12D, *TET2* Q114X, *TET2* G1370R, *FLT3*-ITD
48*	WT	
49*	*BRAF* N486_P490 deletion	*NRAS* Q61R
50	*BRAF* V600E	*NRAS* G12D
51*	*BRAF* V600E	
52*	*BRAF* N486_P490 deletion	
53	*BRAF* N486_P490 deletion	
54	WT	
55	*NRAS* Q61R	
56*	*BRAF* V600E	
57	*MAP2K1* E102_I103 deletion	*IDH1* G105D
58*	*NRAS* Q61K	
59*	*BRAF* V600E	*NRAS* Q61K
60*	*MAP2K1* Q56P	
61	*BRAF* V600E	
62*	*BRAF* N486_P490 deletion	
63	*KRAS* G12S	
64	*BRAF* N486_P490 deletion	
65	WT	
66*	*BRAF* N486_P490 deletion	
67*	WT	
68*	*MAP2K1* K57N	
69	WT	

* Patients with PLCH at diagnosis (n=50).

Abbreviations: LCH: Langerhans cell histiocytosis; NGS: next-generation sequencing; WT: wild type; ITD: internal tandem duplication.

Table 3. Comparison of clinical features at diagnosis of the 117 LCH patients according to the *BRAF*^{V600E} status of their lesions.

Characteristic	*BRAF*^{V600E} (n=43)	Without *BRAF*^{V600E} (n=74)	p-value
Female	20 (46.5)	36 (48.6)	0.85
Age, years median [IQR]	38.0 [26.6-50.0]	35.2 [25.0-45.8]	0.24
MS, n (%)	12 (27.9)	26 (35.1)	0.54
Number of involved organs* 1 2 3 4	 31 (72) 7 (16.3) 2 (4.7) 3 (7)	 48 (64.9) 16 (21.6) 6 (8.1) 4 (5.4)	0.78
Lung	31 (72.1)	52 (70.3)	1.00
Bone	10 (23.3)	23 (31.1)	0.40
Pituitary†	6 (13.9)	10 (13.5)	1.00
Skin	7 (16.3)	12 (16.2)	1.00
Lymph node	3 (7)	6 (8.1)	1.00

* Risk organ involvement (liver or haematological involvement) and central nervous system localisation were not assessed, as they concerned only 3 patients each in the entire study population.

† Diabetes insipidus (associated or not with anterior hypophysis deficiency).

Abbreviations: LCH: Langerhans cell histiocytosis; IQR: interquartile range; MS: multisystem.

Table 4. Multivariable analysis of factors associated with pulmonary outcome among the 83 PLCH patients at diagnosis*.

Characteristic	HR (95%CI)	p-value
Age at diagnosis	1.03 (1.00 to 1.05)	0.083
Airflow obstruction	2.00 (1.05 to 3.84)	0.036

* Airflow obstruction: FEV_1/FVC ratio <70%;

Abbreviations: PLCH: pulmonary Langerhans cell histiocytosis; HR: hazard ratio; CI: confidence interval.

Figure legends

Figure 1. Flow chart of the 117 LCH patients included in the study.

Abbreviations. LCH: Langerhans cell histiocytosis; PLCH: pulmonary Langerhans cell histiocytosis.

Figure 2. Mutational landscape in 69 LCH patients whose lesions were widely genotyped by NGS and pyrosequencing for *BRAF* deletions. The basic plot was created using cBioPortal. The altered genes are listed on the left side of the diagram. *: mutation; del: small deletion; green square: missense mutation; brown square: in-frame mutation; black square: truncating mutation; grey rectangle: no alteration detected.

All *BRAF* mutations are $BRAF^{V600E}$ mutations except one, which is a $BRAF^{G469A}$ mutation. The *BRAF*, *NRAS*, *MAP2K1*, *KRAS*, *EGFR, DUSP4, ERBB2*, *ERBB4* and *MET* genes belong or are linked to the MAPK pathway, and *IDH1* and *TET2* belong to the family of epigenetic modifiers.

Abbreviations. LCH: Langerhans cell histiocytosis; NGS: next-generation sequencing; MAPK: mitogen-activated protein kinases.

Figure 3. Distribution of MAPK alterations among the 69 LCH patients whose lesions were evaluated by NGS and pyrosequencing for *BRAF* deletions. Pie chart illustrating the percentages of identified MAPK alterations. *MAP2K1* comprises both mutations and deletions. Concurrent genomic alterations were not recorded.

Abbreviations: MAPK: mitogen-activated protein kinases; LCH: Langerhans cell histiocytosis; NGS: next-generation sequencing.

Figure 4. Cumulative incidence of disease progression among the 69 LCH patients whose lesions were widely genotyped, according to the different MAPK alterations identified. $BRAF^{V600E}$ (n=25); other *BRAF* alterations (n=21; *BRAF* deletions n=19, other n=2); non-*BRAF*

alterations (n=14; *MAP2K1* n=10; *NRAS/KRAS* n=4) and wild-type (n=9). Solid line: *BRAF*^{V600E} mutation; dotted line: other *BRAF* alterations; dashed line: non-*BRAF* alterations; dash dotted line: Wild-type.

Abbreviations: LCH: Langerhans cell histiocytosis; MAPK: mitogen-activated protein kinases.

Figure 5. Cumulative incidence of disease progression among all LCH patients whose lesions were genotyped for the presence of the *BRAF*^{V600E} mutation. (a) Disease progression among the 117 patients tested according to the presence or absence of the *BRAF*^{V600E} mutation, based on the assessment of the global outcome of their LCH localisations. (b) Same comparison for the 83 PLCH patients at diagnosis who experienced pulmonary progression during the study period. Solid line: *BRAF*^{V600E}; dashed line: no *BRAF*^{V600E} mutation.

Abbreviations: LCH: Langerhans cell histiocytosis. PLCH: pulmonary Langerhans cell histiocytosis.

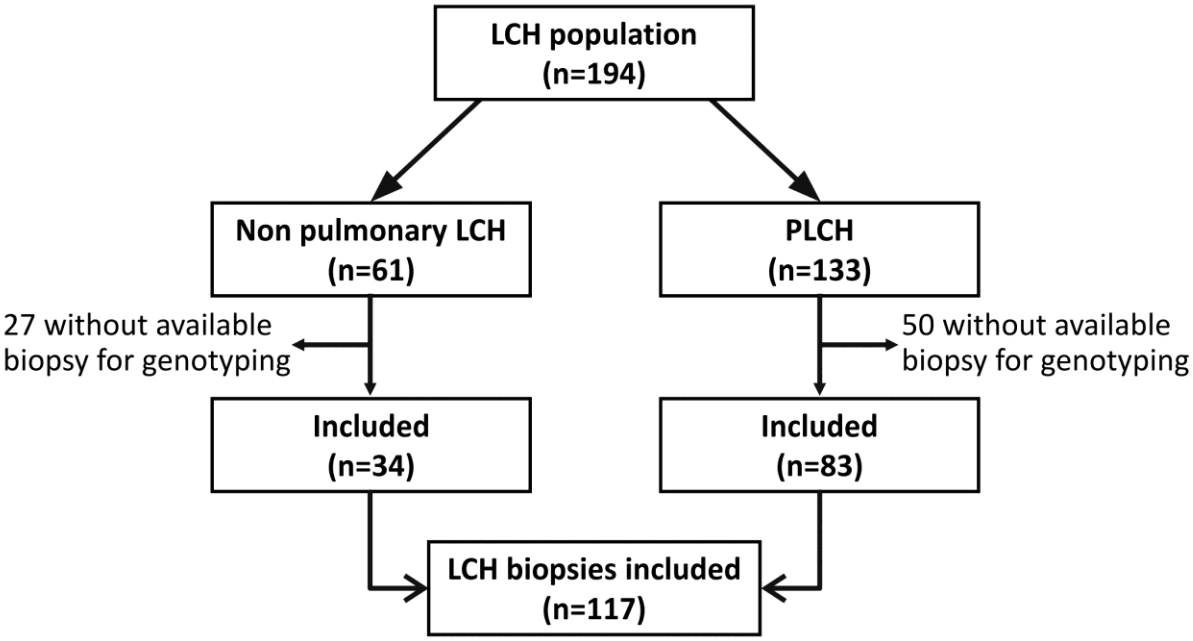
LCH population
(n=194)
Non pulmonary LCH
(n=61)
PLCH
(n=133)
27 without available
biopsy for genotyping
50 without available
biopsy for genotyping
Included
(n=34)
Included
(n=83)
LCH biopsies included
(n=117)

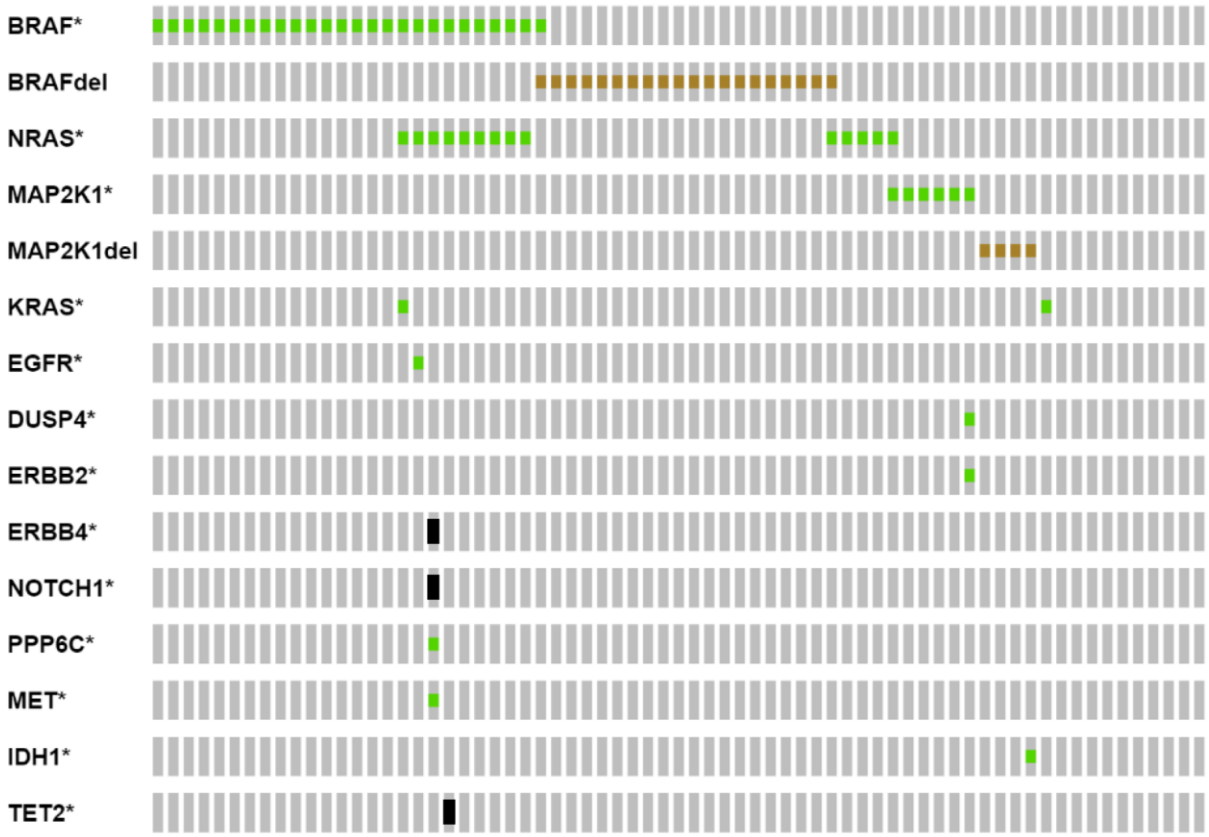
BRAF*
BRAFdel
NRAS*
MAP2K1*
MAP2K1del
KRAS*
EGFR*
DUSP4*
ERBB2*
ERBB4*
NOTCH1*
PPP6C*
MET*
IDH1*
TET2*

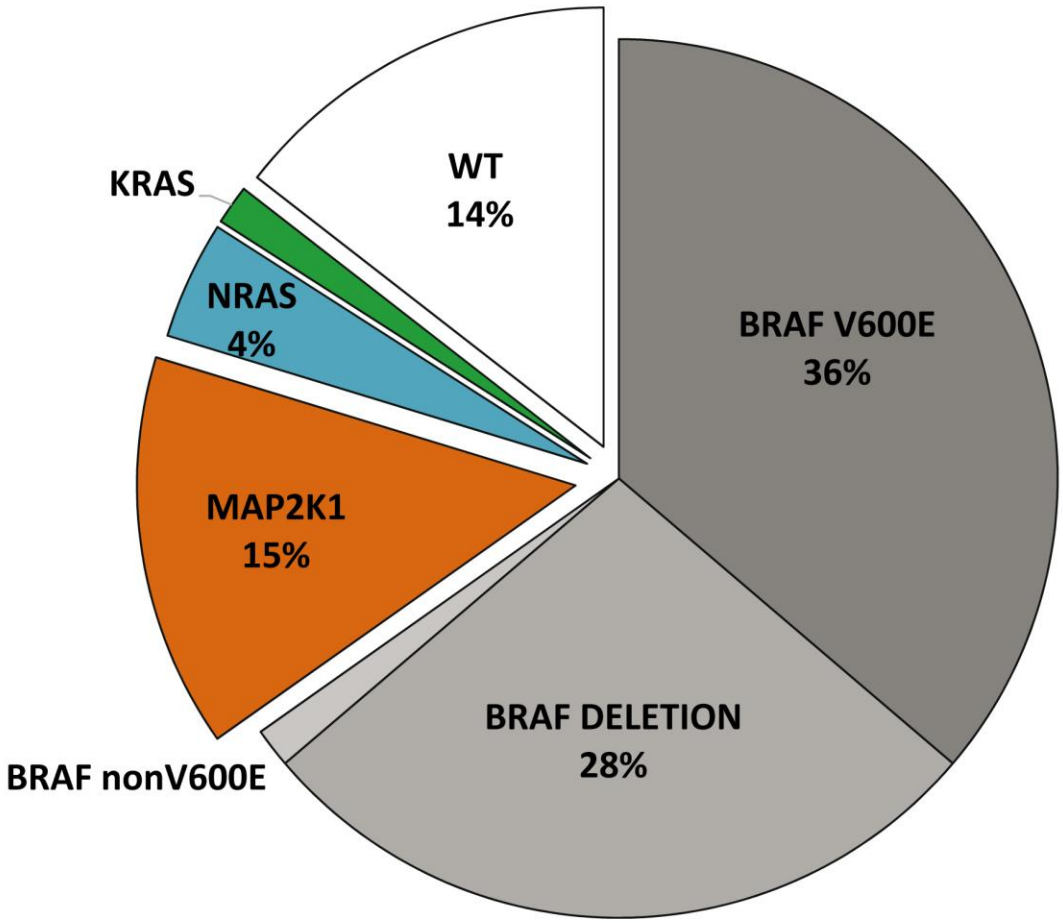
WT
14%
KRAS
NRAS
4%
BRAF V600E
36%
MAP2K1
15%
BRAF DELETION
28%
BRAF nonV600E

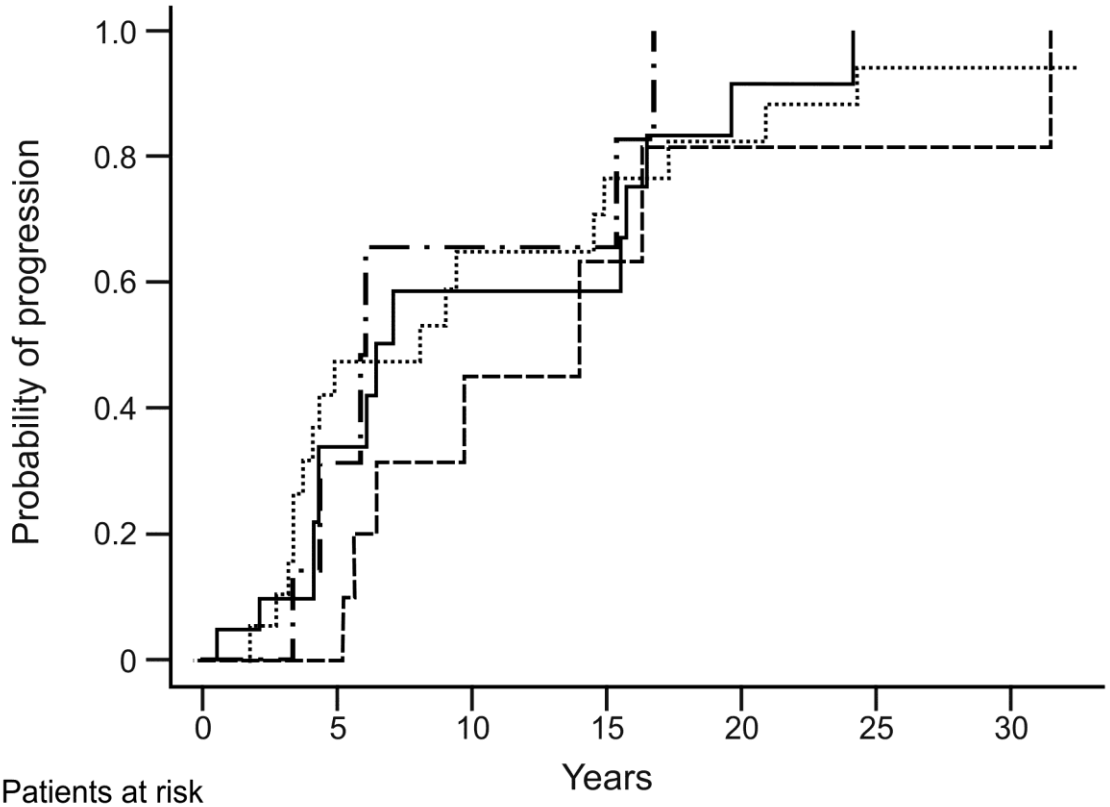

Patients at risk

BRAF^{V600E}	25	11	5	5	1	0	0
Other *BRAF*	21	10	6	4	3	1	1
Non-*BRAF*	14	10	3	2	1	1	1
Wild-type	9	4	2	2	0	0	0

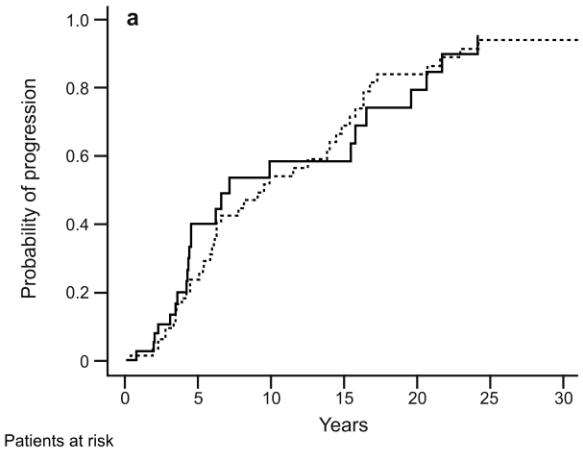

Patients at risk

BRAF V600E	43	18	9	7	3	0	0
No-*BRAF* V600E	74	40	18	12	6	2	2

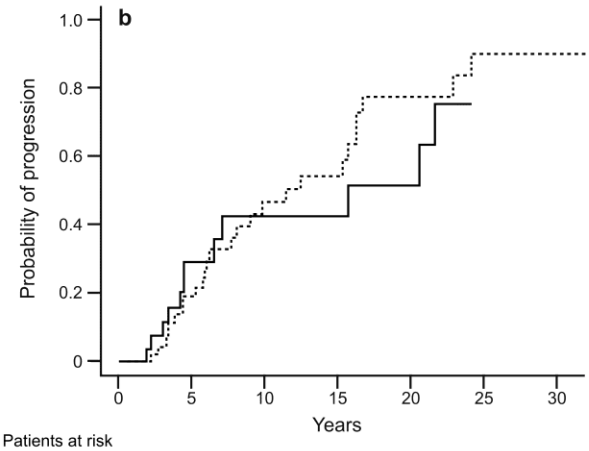

Patients at risk

BRAF V600E	31	15	7	5	3	0	0
No-*BRAF* V600E	52	29	13	8	4	1	1

Supplementary material

Genetic Landscape of Adult Langerhans Cell Histiocytosis with Lung Involvement

Fanélie Jouenne, Sylvie Chevret, Emmanuelle Bugnet, Emmanuelle Clappier, Gwenaël Lorillon, Véronique Meignin, Aurélie Sadoux, Shannon Cohen, Alain Haziot, Alexandre How-Kit, Caroline Kannengiesser, Céleste Lebbé, Dominique Gossot, Samia Mourah, Abdellatif Tazi

Supplementary methods

Study population

The 117 adult LCH patients included in the study were part of a cohort of 194 patients PLCH seen at our centre during the same period. Supplementary Tables 1 and 2 show the characteristics at diagnosis of the patients included and not included in the study.

DNA extraction

DNA was extracted as previously described [1]. Briefly, DNA was extracted from patient peripheral blood mononuclear cells (PBMCs) and tissue samples using the Maxwell RSC DNA FFPE kit and Maxwell RSC Blood DNA (Promega, Charbonnières-les-Bains, France) according to the manufacturer's instructions. DNA concentration was quantified using a Qubit^{tm} dsDNA Hs Assay Kit (Qiagen, Courtaboeuf, France) to ensure accurate starting concentrations.

Whole-exome sequencing (WES)

Exome capture was performed on the genomic platform of the IMAGINE Institute (Paris, France) using a combination of kits and protocols from Rubicon Genomics (Saint-Germain-en-Laye, France) and Agilent Technologies (Les Ulis, France).

Illumina-compatible barcoded genomic DNA libraries were constructed according to the manufacturer’s sample preparation protocol (ThruPLEX DNA-Seq Kit, Rubicon Genomics). Capture by hybridization was performed with an equimolar pool of two Rubicon precapture barcoded libraries using the SureSelect Human All Exon Kit 58 Mb V6 (Agilent Technologies).

Pools of exome libraries were sequenced using the HiSeq2500 platform (Illumina, San Diego, CA, USA), generating paired-end reads.

Whole-exome sequencing data analysis

After demultiplexing, sequences were aligned to the reference human genome (NCBI build37/hg19 version) using Burrows-Wheeler Aligner (BWA) [2]. Downstream processing was carried out with the Genome Analysis Toolkit (GATK), SAM tools, and Picard tools following documented best practices (http://www.broadinstitute.org/gatk/guide/topic?name=best-practices). Variant calls were made with the GATK HaplotypeCaller. All variants with a read coverage $\leq 2X$ and a Phred-scaled quality of ≤ 20 were filtered out. The annotation process was based on the latest release of the Ensembl database [3].

Variants were annotated and analysed using Polyweb software (http://www.polyweb.fr/) and Alamut software (Interactive Biosoftware, Rouen, France).

For the 14 LCH lesions, the exome sequencing data were filtered by 1) removing all germline variants by detection in PBMCs, used as matched control samples; 2) excluding all variants referenced with a frequency $\geq 1\%$ in public databases (dbSNP, 1000 Genomes, EVS, ExAC and GnomAD); 3) keeping variants such as missense, stop-gained, start/stop loss, splice (acceptor, donor or splice region), frameshift or in-frame indel variants; 4) excluding variants predicted as tolerated by two types of prediction software implemented in the Polyweb interface, Polyphen-2 [4] and SIFT [5]; and 5) evaluating the position of the variant in a sequence encoding functional domains, as well as nucleotide and amino acid conservation through the evolution of species. Each mutation was also confirmed as exclusively somatic using BAM files and

Integrative Genomics Viewer (IGV) (http://software.broadinstitute.org/software/igv/); mutations present in any PBMCs samples were excluded.

To identify mutations with low allelic frequency in known oncogene hotspots [6] that may have been missed by our variant calling pipeline, we conducted a deeper BAM file analysis using IGV (without taking into account the filters used with the Polyweb pipeline).

WES datasets are available upon request.

Next-generation sequencing

Next-generation sequencing (NGS) custom-designed panel and data analysis

Targeted sequencing was performed with a customized AmpliSeq™ panel (Thermo Fisher Scientific, Les Ulis, France) targeting 74 genes, including genes involved in the mitogen-activated protein kinases (MAPK), phosphoinositide-3-kinase (PI3K), cell cycle, and tyrosine kinase receptor signalling pathways (Supplementary Table 4) [7-12]. Sequencing amplicon libraries were synthesised from 50 ng of genomic DNA isolated from frozen tissue samples or formalin-fixed paraffin-embedded (FFPE) tissue using an Ion AmpliSeq™ Library Kit 2.0 (Thermo Fisher Scientific) and were indexed with the Ion Xpress Barcode Adapters Kit (Life Technologies, Carslbad, CA, USA) following the manufacturers' instructions. The library amplicon pool was sequenced with the Ion PGM™ Sequencer (Thermo Fisher Scientific). The mean depth was 1647X, and the coverage at a minimum depth of 100X was 94.5%. Data analysis was performed using the Torrent Suite Software v5.8.0 (Thermo Fisher Scientific). Annotation and interpretation of variants were performed using ANNOVAR through the Galaxy-Curie interface (https://galaxy-public.curie.fr/root), IGV and Alamut.

Next-generation sequencing (NGS) for myeloid haematological disorders

Targeted sequencing of all exons of 78 genes recurrently involved in myeloid haematological malignancies was performed using a customized SureSelect™ (Agilent Technologies) capture panel (Supplementary Table 5) [13-15]. Libraries were prepared from 200 ng of genomic DNA isolated from frozen tissue samples according to the manufacturer's instructions and sequenced on MiSeq using Illumina reagents. The mean depth was 364X, and the coverage at a minimum depth of 100X was 96%.

Data analysis was performed using an in-house pipeline using GATK, Varscan and Pindel tools. Interpretation of variants was performed with the aid of human genome databases, the COSMIC database, prediction algorithms (including SIFT and PolyPhen-2) and a literature review.

Pyrosequencing for detection of BRAF exon 12 deletions

Targeted analysis of *BRAF* exon 12 deletions was performed using a pyrosequencing custom-designed assay on a PyroMark Q48 instrument (Qiagen, Hilden, Germany). PCR amplification primers and the sequence content analysed were designed by Qiagen; primer sequences and PCR conditions are available upon request.

The pyrosequencing validation method was conducted and compared with Sanger sequencing by testing DNA samples with a *BRAF* exon 12 deletion or wild type. Sanger sequencing primers were designed with Primer-BLAST (https://www.ncbi.nlm.nih.gov/tools/primer-blast/) and are available upon request. Pyrosequencing showed 100% concordance with known genotypes as identified by Sanger

sequencing. In addition, the identification of *BRAF* exon 12 deletion by pyrosequencing was also concordant with WES analysis (n=6 samples). An example of a *BRAF* exon 12 deletion (N486_P490) result from Sanger sequencing, WES and pyrosequencing is shown in Supplementary Figure 2.

Supplementary tables

Supplementary Table 1. Characteristics at diagnosis of the PLCH patients included in the study (n=83) and those with histologically proven PLCH whose biopsy was not available for genotyping (n=50).

Characteristic	n=83	n=50	p-value
Age, years, median, [IQR]	36.0 [25.4; 45.6]	33.5 [23.7; 42.4]	0.49
Female, n (%)	40 (48.2)	28 (56)	0.47
SS LCH	51 (61.5)	35 (70)	0.35
Active smokers Ex-smokers Non-smokers	65 (78.3) 16 (19.3) 2 (2.4)	41 (82) 5 (10) 4 (8)	0.16
Pneumothorax, n (%)	20 (24)	10 (20)	0.67
TLC, mean ± SD, % predicted	93 [86.75; 106]	92 [82.5; 105]	0.68
FVC, % predicted	88 [73; 97]	87 [75; 97]	0.90
RV, % predicted	114 [88; 145]	114.5 [92; 124]	0.67
FEV_1, % predicted	84 [60; 95]	83 [67; 92]	0.99
FEV_1/FVC, %	77 [68.5; 83.5]	79 [72; 82]	0.86
D_{LCO}, % predicted	58 [44.5; 71]	60 [42; 68.5]	0.71

Abbreviations: PLCH: pulmonary Langerhans cell histiocytosis; IQR: interquartile range; SS: single system; LCH: Langerhans cell histiocytosis; TLC: total lung capacity; FVC: forced vital capacity; RV: residual volume; FEV_1: forced expiratory volume in one second; D_{LCO}: diffusing capacity to carbon monoxide.

Supplementary Table 2. Characteristics of the LCH patients without lung involvement at diagnosis included (n=34) and not included (n=27) in the study.

Characteristic	n=34	n= 27	p-value
Age, years, median, [IQR]	39 [26.7; 54.2]	34 [25.9; 45.9]	0.19
Female, n (%)	16 (47.1)	14 (51.8)	0.80
MS LCH	6 (17.6)	4 (14.8)	1.00
Number of involved organs 1 2 3	 28 (82.3) 3 (8.8) 3 (8.8)	 23 (85.2) 3 (11.1) 0 (0)	0.32
Bone	19 (55.9)	20 (74.1)	0.18
DI	3 (8.8)	0 (0)	0.25
Skin	12 (35.3)	5 (18.5)	0.17
Peripheral lymph node	4 (11.8)	1 (3.7)	0.37
Liver	1 (2.9)	1 (3.7)	1.00
CNS	2 (5.9)	0 (0)	0.50
Haematological involvement	0 (0)	2 (7.4)	0.19
Other	1 (2.9)	1 (3.7)	0.69

Abbreviations: LCH: Langerhans cell histiocytosis; IQR: interquartile range; MS: multisystem;

DI: diabetes insipidus; CNS: central nervous system.

Supplementary Table 3. Main clinical features and molecular genotyping experiments performed on tissue lesions from the 117 LCH patients included in the study*.

Patient	Gender	MS/SS	LCH localizations at the time of biopsy†	Tissue specimen	Molecular genotyping
1	F	MS	bone (UF), skin, lymph node	skin	MAPK NGS
2	M	MS	lung, bone (MF), lymph node	lymph node	MAPK NGS, WES, myeloid NGS, CD11c
3	M	MS	lung, DI	lung	MAPK NGS
4	F	SS	lung	lung	MAPK NGS
5	F	SS	lung	lung	MAPK NGS
6	M	SS	lung	lung	MAPK NGS
7	M	MS	lung	lung	MAPK NGS
8	M	SS	lung, bone (UF), DI, skin	skin	MAPK NGS, WES, myeloid NGS
9	M	SS	lung	lung	MAPK NGS, WES, myeloid NGS, CD11c
10	F	SS	lung	lung	MAPK NGS, WES, myeloid NGS, CD11c
11	F	SS	lung	lung	MAPK NGS
12	F	SS	lymph node	lymph node	MAPK NGS
13	F	MS	lung, DI, skin, lymph node	lymph node	MAPK NGS
14	M	MS	lung, bone (MF)	lung	MAPK NGS
15	F	MS	DI, skin, CNS	skin	MAPK NGS
16	M	MS	lung, bone (UF), DI, AHD, skin	skin	MAPK NGS, WES, myeloid NGS
17	M	SS	lung	lung	MAPK NGS
18	F	SS	lung	lung	MAPK NGS
19	M	MS	lung, lymph node, liver	lymph node	MAPK NGS
20	F	SS	lung, bone (UF), DI, AHD, skin	skin	MAPK NGS
21	F	SS	lung	lung	MAPK NGS
22	F	SS	lung	lung	MAPK NGS
23	F	MS	lung, DI	lung	MAPK NGS, WES, myeloid NGS, CD11c
24	F	SS	lung	lung	MAPK NGS
25	F	SS	lung	lung	MAPK NGS

26	M	SS	lung	lung	MAPK NGS
27	M	MS	lung, bone (UF)	lung	MAPK NGS, WES, myeloid NGS, CD11c
28	M	SS	bone (UF)	bone	MAPK NGS
29	M	SS	bone (UF)	bone	MAPK NGS
30	M	MS	lung, skin	lung	MAPK NGS, WES, myeloid NGS, CD11c
31	F	MS	lung, DI, AHD, CNS	lung	MAPK NGS, WES, myeloid NGS, CD11c
32	M	SS	lung	lung	MAPK NGS
33	M	SS	lung	lung	MAPK NGS
34	M	SS	lung	lung	MAPK NGS
35	M	MS	lung, bone (MF)	lung	MAPK NGS
36	M	SS	lung	lung	MAPK NGS
37	M	SS	lung	lung	MAPK NGS
38	F	SS	lung	lung	MAPK NGS
39	M	SS	bone (UF)	bone	MAPK NGS
40	M	SS	lung	lung	MAPK NGS
41	M	MS	lung, DI, AHD, skin	lung	MAPK NGS
42	F	MS	lung, DI	lung	MAPK NGS
43	F	SS	lung	lung	MAPK NGS
44	F	SS	lung	lung	MAPK NGS
45	M	SS	lung	lung	MAPK NGS
46	F	SS	lung	lung	MAPK NGS
47	M	MS	bone (MF), skin, liver	skin	MAPK NGS, WES, myeloid NGS
48	M	SS	lung	lung	MAPK NGS
49	F	SS	lung	lung	MAPK NGS
50	M	SS	bone (MF), skin	skin	MAPK NGS
51	M	SS	lung, bone (UF)	lung	MAPK NGS
52	F	SS	lung, DI, AHD, skin	skin	MAPK NGS
53	M	SS	lung, DI, AHD, skin	skin	MAPK NGS
54	F	MS	DI, AHD, CNS	SNC	MAPK NGS
55	F	SS	bone (MF)	bone	MAPK NGS

56	M	MS	lung, DI, lymph node	lymph node	MAPK NGS, WES, myeloid NGS
57	M	SS	lung, skin, lymph node	lymph node	MAPK NGS, WES, myeloid NGS
58	M	MS	lung, bone (UF)	lung	MAPK NGS
59	F	SS	lung	lung	MAPK NGS, WES, myeloid NGS, CD11c
60	M	SS	lung	lung	MAPK NGS
61	M	SS	bone (UF)	bone	MAPK NGS, WES, myeloid NGS
62	M	SS	lung, skin	skin	MAPK NGS, WES, myeloid NGS
63	M	SS	skin	skin	MAPK NGS
64	F	SS	bone (MF), DI, skin, lymph node	skin	MAPK NGS, WES, myeloid NGS
65	F	SS	skin	skin	MAPK NGS
66	M	SS	lung	lung	MAPK NGS
67	M	SS	lung	lung	MAPK NGS, WES, myeloid NGS, CD11c
68	M	MS	lung, bone (MF), skin	skin	MAPK NGS
69	F	MS	DI, skin	skin	MAPK NGS
70	M	MS	lung, bone (UF), DI, skin	lung	*BRAF* V600E*/NRAS*
71	F	SS	bone (UF)	bone	*BRAF* V600E */NRAS*
72	F	MS	lung, lymph node	lymph node	*BRAF* V600E*/NRAS*
73	M	MS	lung, bone (UF)	bone	*BRAF* V600E*/NRAS*
74	F	SS	lung	lung	*BRAF* V600E*/NRAS*
75	F	SS	lung	lung	*BRAF* V600E*/NRAS*
76	M	SS	bone (UF)	bone	*BRAF* V600E*/NRAS*
77	M	SS	lung	lung	*BRAF* V600E*/NRAS*
78	F	SS	bone (UF)	bone	*BRAF* V600E*/NRAS*
79	M	SS	lung	lung	*BRAF* V600E*/NRAS*
80	M	SS	lung, skin	skin	*BRAF* V600E*/NRAS*
81	F	SS	lung, bone (UF)	bone	*BRAF* V600E*/NRAS*
82	M	MS	lung, bone (UF)	lung	*BRAF* V600E*/NRAS*
83	M	MS	lung, skin	skin	*BRAF* V600E*/NRAS*
84	F	MS	lung, DI, AHD, skin, thyroid	thyroid	*BRAF* V600E*/NRAS*
85	F	MS	lung, bone (UF)	bone	*BRAF* V600E*/NRAS*

86	F	SS	lung	lung	*BRAF* V600E/*NRAS*
87	F	MS	lung, bone (UF), gut	bone	*BRAF* V600E/*NRAS*
88	F	MS	lung, bone (UF)	bone	*BRAF* V600E/*NRAS*
89	F	SS	lung	lung	*BRAF* V600E/*NRAS*
90	F	SS	lung	lung	*BRAF* V600E/*NRAS*
91	F	SS	lung	lung	*BRAF* V600E/*NRAS*
92	F	SS	lung	lung	*BRAF* V600E/*NRAS*
93	M	SS	bone (MF)	bone	*BRAF* V600E/*NRAS*
94	F	SS	lung	lung	*BRAF* V600E/*NRAS*
95	M	MS	lung, bone (UF)	bone	*BRAF* V600E/*NRAS*
96	F	SS	bone (UF)	bone	*BRAF* V600E/*NRAS*
97	M	MS	lung, DI, AHD, skin	skin	*BRAF* V600E/*NRAS*
98	M	SS	bone (UF)	bone	*BRAF* V600E/*NRAS*
99	F	SS	bone (UF)	bone	*BRAF* V600E/*NRAS*
100	F	SS	bone (UF)	bone	*BRAF* V600E/*NRAS*
101	M	MS	lung, bone (UF)	bone	*BRAF* V600E/*NRAS*
102	F	MS	lung, bone (UF)	bone	*BRAF* V600E/*NRAS*
103	M	MS	lung, bone (MF), DI, skin	skin	*BRAF* V600E/*NRAS*, WES, CD11c
104	M	SS	bone (MF)	bone	*BRAF* V600E/*NRAS*
105	M	SS	bone (UF)	bone	*BRAF* V600E/*NRAS*
106	F	MS	lung, DI, skin	skin	*BRAF* V600E/*NRAS*
107	F	SS	lung	lung	*BRAF* V600E/*NRAS*
108	F	SS	lung	lung	*BRAF* V600E/*NRAS*
109	F	SS	lung	lung	*BRAF* V600E/*NRAS*
110	M	SS	skin	skin	*BRAF* V600E/*NRAS*
111	M	SS	lung	lung	*BRAF* V600E/*NRAS*
112	M	SS	skin	skin	*BRAF* V600E/*NRAS*
113	F	MS	lung, DI, AHD, skin	skin	*BRAF* V600E/*NRAS*
114	M	SS	lung	lung	*BRAF* V600E/*NRAS*
115	F	SS	skin	skin	*BRAF* V600E/*NRAS*

116	M	SS	skin	skin	*BRAF* V600E*/NRAS*
117	F	SS	skin	skin	*BRAF* V600E*/NRAS*

*FFPE tissue specimens were available for all patients. WES and myeloid NGS genotyping were performed on additional frozen tissue from the same site. CD11c blood cells were purified by flow cytometry from thawed DMSO-frozen PBMCs.

†For some patients, LCH localizations at the time of biopsy were different from those at the time of diagnosis.

Abbreviations: LCH: Langerhans cell histiocytosis; MS: multisystem; SS: single system; F: female; UF: unifocal; MAPK: mitogen-activated protein kinases; NGS: next-generation sequencing; M: male; MF: multifocal; WES: whole-exome sequencing; DI: diabetes insipidus; CNS: central nervous system; AHD: anterior hypophysis deficiency; FFPE: formalin-fixed paraffin-embedded; PBMCs: peripheral blood mononuclear cells.

Supplementary Table 4. Custom-designed next-generation sequencing panel of 74 genes involved in the MAPK, phosphoinositide-3-kinase, cell cycle, and tyrosine kinase receptor signalling pathways.

ABL1	*CDKN2A*	*ERBB3*	*GNAQ*	*KRAS*	*PDGFRA*	*RAC1*	*TACC1*
AKT1	*CD274*	*ERBB4*	*GRIN2A*	*MAP2K1*	*PDGFRB*	*RAF1*	*TERT*
AKT2	*CTNNB1*	*EZH2*	*GRM3*	*MAP2K2*	*PHLPP1*	*RASA2*	*TRRAP*
AKT3	*CXCR4*	*FBXW7*	*HOXD8*	*MDM2*	*PIK3CA*	*RET*	*WT1*
ALK	*DDR1*	*FERMT3*	*HRAS*	*MET*	*PIK3CG*	*RPS27*	
ARAF	*DDR2*	*FGFR1*	*IDH1*	*MITF*	*PIK3R1*	*SERPINB3*	
BRAF	*DDX3X*	*FGFR2*	*IGF1R*	*MRPS31*	*PIK3R2*	*SNX31*	
BTK	*DUSP4*	*FGFR3*	*JAK2*	*NOTCH1*	*PLCG2*	*STAT3*	
CCND1	*EGFR*	*FLT3*	*KDR*	*NOTCH2*	*PPP6C*	*STK11*	
CDK4	*ERBB2*	*GNA11*	*KIT*	*NRAS*	*PTPN11*	*STK19*	

Supplementary Table 5. Custom-designed next-generation sequencing panel of 78 genes associated with myeloid haematological disorders.

ACD	*BCOR*	*CTCF*	*ETNK1*	*JAK2*	*NF1*	*RUNX1T1*	*STAG2*
AHRR	*BCORL1*	*CUX1*	*ETV6*	*KDM6A*	*NOTCH1*	*SAMD9*	*TERC*
ANKRD26	*BRAF*	*DDX41*	*EZH2*	*KIT*	*NPM1*	*SAMD9L*	*TERT*
APC	*BRCA2*	*DIS3*	*FBXW7*	*KMT2A*	*NRAS*	*SETBP1*	*TET2*
ASXL1	*BRCC3*	*DNAJC21*	*FLT3*	*KMT2D*	*PHF6*	*SF3B1*	*TP53*
ASXL2	*CALR*	*DNMT3A*	*GATA2*	*KRAS*	*PRPF8*	*SMC1A*	*U2AF1*
ATG2B	*CBL*	*DNMT3B*	*GNAS*	*LAMB4*	*PTPN11*	*SMC3*	*WT1*
ATM	*CEBPA*	*DOT1L*	*GSKIP*	*MDM4*	*RAD21*	*SRP72*	*ZRSR2*
ATRX	*CREBBP*	*EP300*	*IDH1*	*MECOM*	*RIT1*	*SRSF2*	
BCL2	*CSF3R*	*ERCC6L2*	*IDH2*	*MPL*	*RUNX1*	*STAG1*	

Supplementary Table 6. Additional mutations identified with myeloid and custom-designed NGS panels.

GENE	Type	Amino acid variant	Genomic variant	Patient number (VAF)	Consequence	Details
ETNK1	SNV	W410X	c.1230G>A	27 (81%)	NS	Activating mutations in ETNK1 kinase domain have been reported in atypical chronic myeloid leukaemia [16]. The functional significance of the C-terminal truncating mutation here is undetermined.
IDH1	SNV	G105D	c.314G>A	57 (10%)	MS	Mutations in *IDH1* (Isocitrate dehydrogenase 1), an epigenetic modifier gene, are described in AML and are mutually exclusive with *TET2* mutations [17]. The *IDH1*^{G105D} mutation is not described functionally. It is located in functional domains of the protein (Isopropylmalate dehydrogenase-like and Isocitrate dehydrogenase NADP-dependent domains) at the level of a strongly conserved amino acid and is predicted to be deleterious with 3/3 prediction algorithms.
DUSP4	SNV	D231N	c.691G>A	5 (12%)	MS	*DUSP4* (Dual Specificity Phosphatase 4 = MAP Kinase Phosphatase 2) negatively regulates members of the MAPK superfamily by dephosphorylation. D231N mutation affects a strongly conserved amino acid located in the phosphatase catalytic domain. It is not described functionally but is predicted to be deleterious based on 2/3 algorithms.
ERBB2	SNV	T791I	c.2372C>T	5 (10%)	MS	Mutation affecting a conserved amino acid, located in the serine-threonine/tyrosine-protein kinase catalytic domain, identified in breast and lung cancers. Not described functionally but predicted to be deleterious based on 2/3 algorithms.
ERBB4	Stop	R838X	c.2512C>T	18 (5%)	NS	Undescribed mutation. Generates a premature stop codon at a strongly conserved site.
NOTCH1	Splice variant	?	c.6181-1G>A	18 (62%)	Alternative splice	Splicing mutation reported in skin cancer [18]. Not described functionally. Probably causes the skip of exon 34, thus truncating the resulting protein.
PPP6C	SNV	P296S	c.886C>T	18 (5%)	MS	*PPP6C* (protein phosphatase 6 catalytic subunit) mutation located on a conserved amino acid in the serine/threonine-specific domain. Undescribed. However, predicted to be deleterious based on 3/3 algorithms.
MET	SNV	S244F	c.731C>T	18 (6%)	MS	Located in the Sema domain and the Tyrosine-protein kinase, HGF/MSP receptor domain. Undescribed but predicted to be deleterious based on 3/3 algorithms.
EGFR	SNV	P753S	c.2257C>T	20 (8%)	MS	Located on a very conserved amino acid in the functional protein kinase domain. Reported in various cancers [19]. Predicted as deleterious based on 2/3 algorithms. **S**KMEL28 and *BRAF*^{V600E} mutant cell lines (which contain *EGFR*^{P753S}, *MITF* amplification, *CCND1* amplification, *CDKN2A* heterozygous deletion and *PTEN* heterozygous deletion) were shown to be sensitive to vemurafenib [20].

Abbreviations: NGS: next-generation sequencing; VAF: variant allele frequency; SNV: single nucleotide variant; NS: nonsense; MS: missense; AML: acute myeloid leukaemia; MAPK: mitogen-activated protein kinases.

Supplementary Table 7. Univariable analyses of factors associated with pulmonary outcome among the 83 PLCH patients at diagnosis.

Characteristic, n	HR	95%CI	p-value
Age, /10 years	1.37	(1.04; 1.80)	0.027
Female (n=40)	1.00		
Male (n=43)	0.95	(0.50; 1.80)	0.88
MS LCH (n=32)	1.00		
SS LCH (n=51)	1.69	(0.83; 3.41)	0.15
Active smokers (n=65)	1.00		
Ex/non-smokers (n=18)	1.30	(0.61; 2.77)	0.50
Pneumothorax			
No (n=63)	1.00		
Yes (n=20)	1.08	(0.53; 2.21)	0.82
TLC, % predicted (n=68)	1.02	(0.99; 1.05)	0.18
FVC, % predicted (n=69)	1.00	(0.98; 1.02)	0.77
RV, % predicted (n=64)	1.01	(1.00; 1.02)	0.054
FEV_1, % predicted (n=73)	0.99	(0.97; 1.01)	0.24
FEV_1/FVC, % (n=69)	0.99	(0.97; 1.00)	0.090
D_{LCO}, % predicted (n=54)	0.99	(0.96; 1.01)	0.25
Restrictive syndrome*			
No (n=59)	1.00		
Yes (n=9)	3.27	(0.92; 11.64)	0.067
Obstructive syndrome			
No (n=39)	1.00		
Yes (n=30)	2.03	(1.03; 4.00)	0.041
Air trapping			
No (n=34)	1.00		
Yes (n=31)	2.03	(0.96; 4.29)	0.063
Impaired D_{LCO}			
No (n=5)	1.00		
Yes (n=49)	1.00	(0.30; 3.35)	1.00

* Restrictive syndrome: TLC<80% of predicted; obstructive syndrome: FEV_1/FVC ratio <70%; air trapping: RV/TLC>120% of predicted; Impaired D_{LCO}: <80% of predicted values.

Abbreviations: PLCH: pulmonary Langerhans cell histiocytosis; HR: hazard ratio; CI: confidence interval; MS: multisystem; LCH: Langerhans cell histiocytosis; SS: single system; TLC: total lung capacity; FVC: forced vital capacity; RV: residual volume; FEV_1: forced expiratory volume in one second; D_{LCO}: diffusing capacity of carbon monoxide.

Supplementary figures

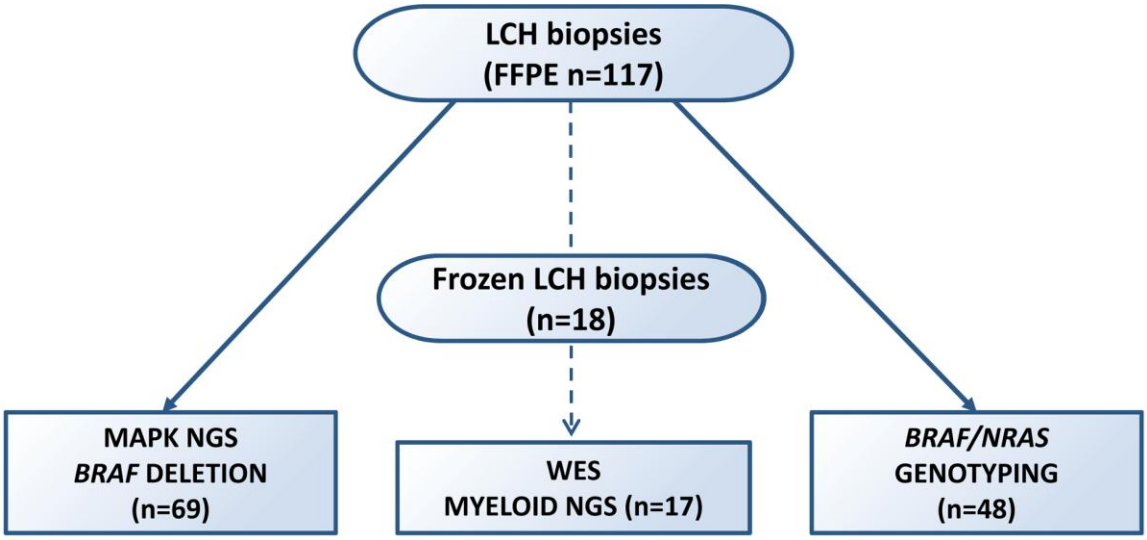

Supplementary Figure 1. Flow chart of genomic-based analysis of LCH lesions.

Abbreviations: LCH, Langerhans cell histiocytosis; FFPE, formalin-fixed paraffin-embedded; MAPK; mitogen-activated protein kinases; NGS; next-generation sequencing; WES; whole-exome sequencing.

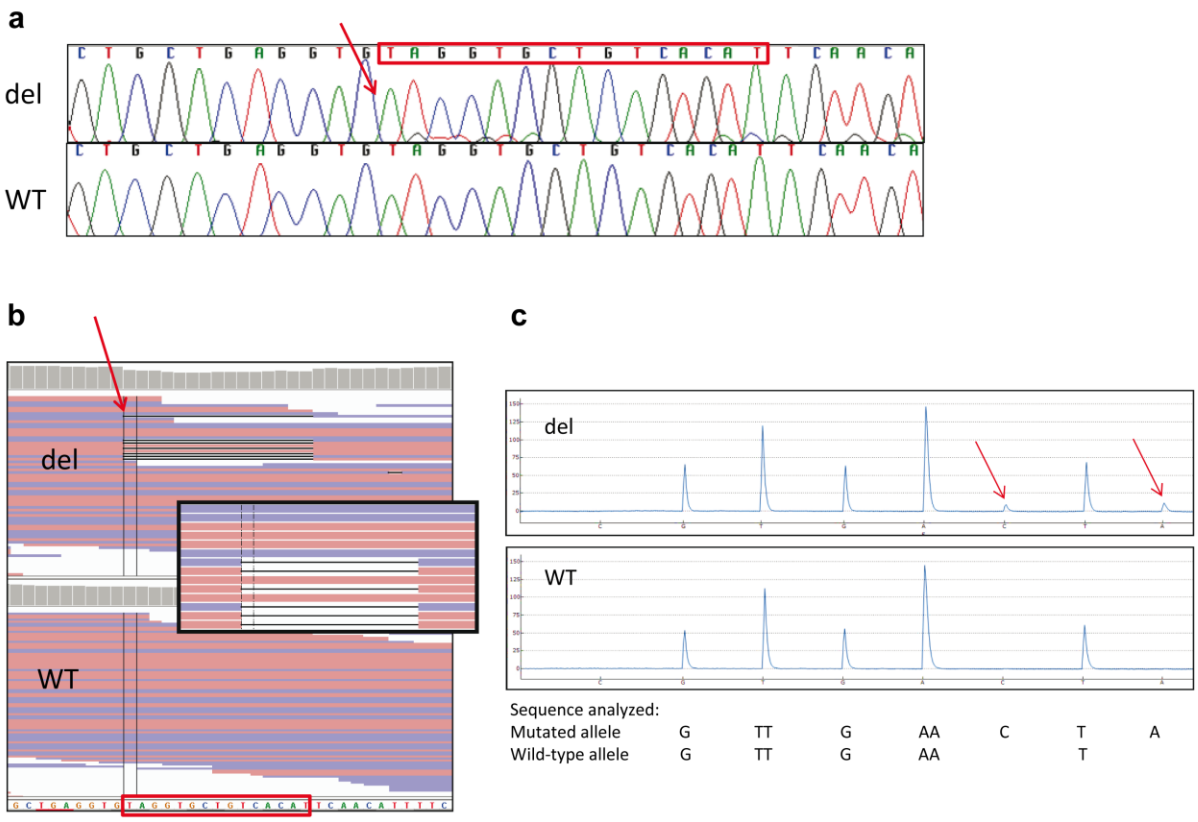

Supplementary Figure 2. An LCH biopsy harbouring a heterozygous *BRAF*$^{N486\_P490}$ deletion in exon 12 evaluated by (a) Sanger sequencing, (b) WES and (c) pyrosequencing.

The deleted DNA sequence is represented in the upper panel, and the wild-type (WT) sequence is represented in the lower panel. Red boxes show the deleted sequence in exon 12 of *BRAF*. In the Sanger electropherograms (a) and the Integrative Genomics Viewer (IGV) visualization of exome sequences (b), the red arrow indicates the starting nucleotide of the deletion. In IGV, black lines represent the *BRAF*$^{N486\_P490}$ deletion (an enlarged view of deleted reads is displayed in the inset). The DNA sequence analysed for *BRAF*$^{N486\_P490}$ deletion detection by pyrosequencing is shown under the pyrograms (c). Heterozygous deletion of the sequence of 15 base pairs leads to a new mutated sequence with a new C and A (red arrows).

Abbreviations: del, deletion; WT, wild type; LCH, Langerhans cell histiocytosis; WES; whole-exome sequencing.

Supplementary references

1. Mourah S, How-Kit A, Meignin V, Gossot D, Lorillon G, Bugnet E, Mauger F, Lebbe C, Chevret S, Tost J, Tazi A. Recurrent NRAS mutations in pulmonary Langerhans cell histiocytosis. Eur Respir J 2016; 47: 1785-1796.
2. Li H, Durbin R. Fast and accurate long-read alignment with Burrows-Wheeler transform. Bioinformatics 2010; 26: 589-595.
3. Yates A, Akanni W, Amode MR, Barrell D, Billis K, Carvalho-Silva D, Cummins C, Clapham P, Fitzgerald S, Gil L, Giron CG, Gordon L, Hourlier T, Hunt SE, Janacek SH, Johnson N, Juettemann T, Keenan S, Lavidas I, Martin FJ, Maurel T, McLaren W, Murphy DN, Nag R, Nuhn M, Parker A, Patricio M, Pignatelli M, Rahtz M, Riat HS, Sheppard D, Taylor K, Thormann A, Vullo A, Wilder SP, Zadissa A, Birney E, Harrow J, Muffato M, Perry E, Ruffier M, Spudich G, Trevanion SJ, Cunningham F, Aken BL, Zerbino DR, Flicek P. Ensembl 2016. Nucleic Acids Res 2016; 44: D710-D716.
4. Adzhubei IA, Schmidt S, Peshkin L, Ramensky VE, Gerasimova A, Bork P, Kondrashov AS, Sunyaev SR. A method and server for predicting damaging missense mutations. Nat Methods 2010; 7: 248-249.
5. Kumar P, Henikoff S, Ng PC. Predicting the effects of coding non-synonymous variants on protein function using the SIFT algorithm. Nat Protoc 2009; 4: 1073-1081.
6. Durham BH, Diamond EL, Abdel-Wahab O. Histiocytic neoplasms in the era of personalized genomic medicine. Curr Opin Hematol 2016; 23: 416-425.
7. Badalian-Very G, Vergilio JA, Degar BA, Rodriguez-Galindo C, Rollins BJ. Recent advances in the understanding of Langerhans cell histiocytosis. Br J Haematol 2010; 156: 163-172.

8. Cancer Genome Atlas Network. Genomic classification of cutaneous melanoma. Cell 2015; 161: 1681-1696.

9. Chakraborty R, Hampton OA, Shen X, Simko SJ, Shih A, Abhyankar H, Lim KP, Covington KR, Trevino L, Dewal N, Muzny DM, Doddapaneni H, Hu J, Wang L, Lupo PJ, Hicks MJ, Bonilla DL, Dwyer KC, Berres ML, Poulikakos PI, Merad M, McClain KL, Wheeler DA, Allen CE, Parsons DW. Mutually exclusive recurrent somatic mutations in MAP2K1 and BRAF support a central role for ERK activation in LCH pathogenesis. Blood 2014; 124: 3007-3015.

10. Hodis E, Watson IR, Kryukov GV, Arold ST, Imielinski M, Theurillat JP, Nickerson E, Auclair D, Li L, Place C, Dicara D, Ramos AH, Lawrence MS, Cibulskis K, Sivachenko A, Voet D, Saksena G, Stransky N, Onofrio RC, Winckler W, Ardlie K, Wagle N, Wargo J, Chong K, Morton DL, Stemke-Hale K, Chen G, Noble M, Meyerson M, Ladbury JE, Davies MA, Gershenwald JE, Wagner SN, Hoon DS, Schadendorf D, Lander ES, Gabriel SB, Getz G, Garraway LA, Chin L. A landscape of driver mutations in melanoma. Cell 2012; 150: 251-263.

11. Nelson DS, van Halteren A, Quispel WT, van den Bos C, Bovee JV, Patel B, Badalian-Very G, van Hummelen P, Ducar M, Lin L, MacConaill LE, Egeler RM, Rollins BJ. MAP2K1 and MAP3K1 mutations in Langerhans cell histiocytosis. Genes Chromosomes Cancer 2015; 54: 361-368.

12. van Allen EM, Wagle N, Sucker A, Treacy DJ, Johannessen CM, Goetz EM, Place CS, Taylor-Weiner A, Whittaker S, Kryukov GV, Hodis E, Rosenberg M, McKenna A, Cibulskis K, Farlow D, Zimmer L, Hillen U, Gutzmer R, Goldinger SM, Ugurel S, Gogas HJ, Egberts F, Berking C, Trefzer U, Loquai C, Weide B, Hassel JC, Gabriel SB, Carter

SL, Getz G, Garraway LA, Schadendorf D, Dermatologic Cooperative Oncology Group of Germany. The genetic landscape of clinical resistance to RAF inhibition in metastatic melanoma. Cancer Discov 2014; 4: 94-109.

13. Lindsley RC, Mar BG, Mazzola E, Grauman PV, Shareef S, Allen SL, Pigneux A, Wetzler M, Stuart RK, Erba HP, Damon LE, Powell BL, Lindeman N, Steensma DP, Wadleigh M, DeAngelo DJ, Neuberg D, Stone RM, Ebert BL. Acute myeloid leukemia ontogeny is defined by distinct somatic mutations. Blood 2015; 125: 1367-1376.

14. Papaemmanuil E, Gerstung M, Bullinger L, Gaidzik VI, Paschka P, Roberts ND, Potter NE, Heuser M, Thol F, Bolli N, Gundem G, van Loo P, Martincorena I, Ganly P, Mudie L, McLaren S, O'Meara S, Raine K, Jones DR, Teague JW, Butler AP, Greaves MF, Ganser A, Dohner K, Schlenk RF, Dohner H, Campbell PJ. Genomic classification and prognosis in acute myeloid leukemia. N Engl J Med 2016; 374: 2209-2221.

15. Papaemmanuil E, Gerstung M, Malcovati L, Tauro S, Gundem G, van Loo P, Yoon CJ, Ellis P, Wedge DC, Pellagatti A, Shlien A, Groves MJ, Forbes SA, Raine K, Hinton J, Mudie LJ, McLaren S, Hardy C, Latimer C, Porta MGD, O'Meara S, Ambaglio I, Galli A, Butler AP, Walldin G, Teague JW, Quek L, Sternberg A, Gambacorti-Passerini C, Cross NC, Green AR, Boultwood J, Vyas P, Hellstrom-Lindberg E, Bowen D, Cazzola M, Stratton MR, Campbell PJ, Chronic Myeloid Disorders Working Group of the International Cancer Genome Consortium. Clinical and biological implications of driver mutations in myelodysplastic syndromes. Blood 2013; 122: 3616-3627.

16. Gambacorti-Passerini CB, Donadoni C, Parmiani A, Pirola A, Redaelli S, Signore G, Piazza V, Malcovati L, Fontana D, Spinelli R, Magistroni V, Gaipa G, Peronaci M, Morotti A, Panuzzo C, Saglio G, Usala E, Kim DW, Rea D, Zervakis K, Viniou N,

Symeonidis A, Becker H, Boultwood J, Campiotti L, Carrabba M, Elli E, Bignell GR, Papaemmanuil E, Campbell PJ, Cazzola M, Piazza R. Recurrent ETNK1 mutations in atypical chronic myeloid leukemia. Blood 2015; 125: 499-503.

17. Shih AH, Abdel-Wahab O, Patel JP, Levine RL. The role of mutations in epigenetic regulators in myeloid malignancies. Nat Rev Cancer 2012; 12: 599-612.

18. Pickering CR, Zhou JH, Lee JJ, Drummond JA, Peng SA, Saade RE, Tsai KY, Curry JL, Tetzlaff MT, Lai SY, Yu J, Muzny DM, Doddapaneni H, Shinbrot E, Covington KR, Zhang J, Seth S, Caulin C, Clayman GL, El-Naggar AK, Gibbs RA, Weber RS, Myers JN, Wheeler DA, Frederick MJ. Mutational landscape of aggressive cutaneous squamous cell carcinoma. Clin Cancer Res 2014; 20: 6582-6592.

19. Ganesan P, Ali SM, Wang K, Blumenschein GR, Esmaeli B, Wolff RA, Miller VA, Stephens PJ, Ross JS, Palmer GA, Janku F. Epidermal growth factor receptor P753S mutation in cutaneous squamous cell carcinoma responsive to cetuximab-based therapy. J Clin Oncol 2016; 34: e34-e37.

20. Sondergaard JN, Nazarian R, Wang Q, Guo D, Hsueh T, Mok S, Sazegar H, MacConaill LE, Barretina JG, Kehoe SM, Attar N, von Euw E, Zuckerman JE, Chmielowski B, Comin-Anduix B, Koya RC, Mischel PS, Lo RS, Ribas A. Differential sensitivity of melanoma cell lines with BRAFV600E mutation to the specific raf inhibitor PLX4032. J Transl Med 2010; 8: 39.